1964-1967 PhD in Physics. Fellowships from CNR. During this period most important papers appeared in *Science and Nature (Lond.)* in the field of Artificial Intelligence.

1968-1979 Research Associate of Consiglio Nazionale delle Ricerche (CNR) at the Institute of Cypernetics and Biophysics of CNR, Camogli, Italy.

1972 Lecturer (libera docenza) in Cybernetics and Information Theory, University of Genoa

1973-1975 Evaluation of ion channel conductance from power spectral density analysis of nerve membrane currents. Visiting professor at Emory University, Dept.of Anatomy, Atlanta, Georgia, USA.

1979-82 Studies on the effect of pH changes and scorpion toxins in the ion channels of nerve membrane *Nature (Lond.), vol. 287 and 296*.

1980 Full professor of Physiology at the University of Ferrara.

1982 Professor of Physiology at the University of Milano.

Molecular Shape and Odour : Pattern Analysis by PAPA

(*Reprinted from Nature, Vol. 216, No. 5120, pp. 1084–1087, December 16, 1967*)

by

J. E. AMOORE

Western Regional Research Laboratory,
Agricultural Research Service,
US Department of Agriculture,
Albany, California

G. PALMIERI
E. WANKE

Istituto di Fisica, Università degli Studi,
Genoa, Italy

The PAPA pattern recognition machine, consisting of an image dissector and computer, can rapidly and accurately make comparative measurements of molecular model silhouettes. This will be most useful for research on the stereochemical specificity of the sense of smell.

Ant Alarm Pheromone Activity:
Correlation with Molecular Shape by Scanning Computer

John E. Amoore, Guido Palmieri, Enzo Wanke, Murray S. Blum

Reprinted from
19 September 1969, volume 165, pages 1266-1269

SCIENCE

Ant Alarm Pheromone Activity:
Correlation with Molecular Shape by Scanning Computer

Abstract. *The ant* Iridomyrmex pruinosus *utilizes 2-heptanone as an alarm pheromone. The activities of 49 ketones and 35 nonketones as alarm pheromones for this species were determined. The molecular shapes of these compounds were assessed by submitting silhouette photographs of their molecular models to a pattern recognition machine. A highly significant correlation exists between molecular shape and alarm activity.*

Reprinted from Nature, Vol. 296, No. 5852, pp. 90-91, 4 March 1982

Selective blockage of voltage-dependent K^+ channels by a novel scorpion toxin

Emilio Carbone*, Enzo Wanke†, Gianfranco Prestipino*, Lourival D. Possani‡ & Alfred Maelicke§

Blocking agents of high selectivity are crucial in defining both physiologically and biochemically the molecular components that control membrane excitability. To obtain such probes for voltage-dependent ion channels, we have examined the venom of several American scorpions for the presence of polypeptide neurotoxins having the required properties. We report here that

Reprinted from Nature, Vol 287, No. 5777, pp. 62-63, September 4 1980

The sodium channel and intracellular H^+ blockage in squid axons

Enzo Wanke, Emilio Carbone & Pier Luigi Testa

Sodium channels in plasma membranes can be blocked by a large variety of toxins[1] and local anaesthetics[2]. This property, however, is not confined to relatively large molecules. For instance, extracellularly applied small ions like hydrogen may also prevent the passive transport of permeant cations across open Na^+ channels[3–6]. A typical feature of this phenomenon[3,5] is

A growing number of experimental studies have used patch-clamp amplifiers (PCAs) in the current-clamp (CC) mode to investigate classical excitability. In this paper we show that the measurements obtained in this way are affected by errors due to the electronic design of the PCA input section. We present experimental evidence of such errors, and demonstrate that they derive from PCA current absorption. Moreover, we propose a new PCA input-circuit configuration for the CC mode, which is suitable for accurately recording physiological voltage signals and is perfectly compatible with the standard voltage-clamp mode.

trends in NEUROSCIENCES
December 1996, Vol. 19, No. 12 (222)

Volume 489 • 2

THE JOURNAL OF PHYSIOLOGY

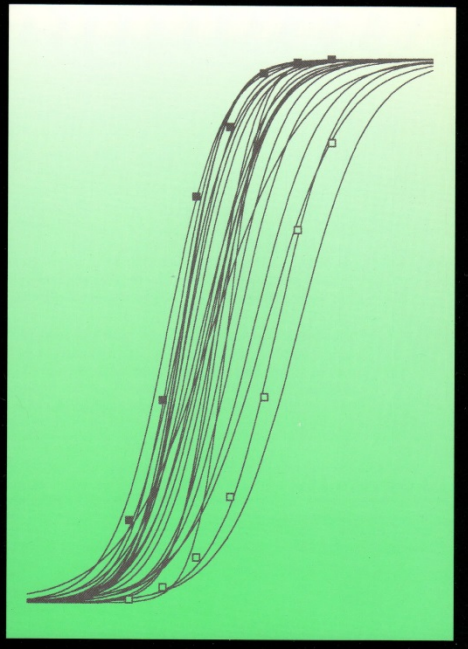

December 1st 1995

A publication of The Physiological Society

THE FASEB JOURNAL

A Multidisciplinary Resource for the Life Sciences

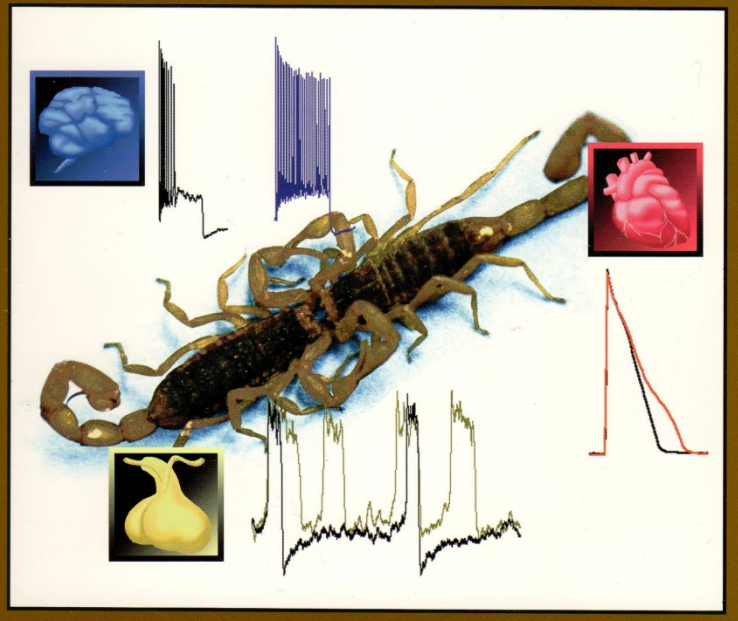

TOXIN TO ERG K^+ CHANNELS

Also in this issue: Caspase activation in B cells
Regulation of MMP in tumor invasion • Cyclin E in human cancers
Spawning pheromone responses in *nereis*

Official Publication of the Federation of American Societies for Experimental Biology
May 1999, Volume 13, Number 8

Statistical methods in studies of firing activity recorded in neuronal networks *7-23*

Do you remember the meaning of :

ACF = autocorrelation function

CV = coefficient of variation = standard deviation / mean

CV2 or **CV^2** = squared CV

Fano factor (FF) = spike-counts variance / mean

We will see the following topics:

Knowing neurons from inside or outside
Principles of recordings
Suggestions from models
Electrodes recording more than one neuron (a unit) up to….
Sorting criteria & Principal Component Analysis in 3D
K-means clustering classification, Outliers *vs* Mahalanobis threshold
Identifying excitatory and inhibitory cells: statistical & physiological methods
Autocorrelation function and cross-correlation
Bursting properties and classification criteria

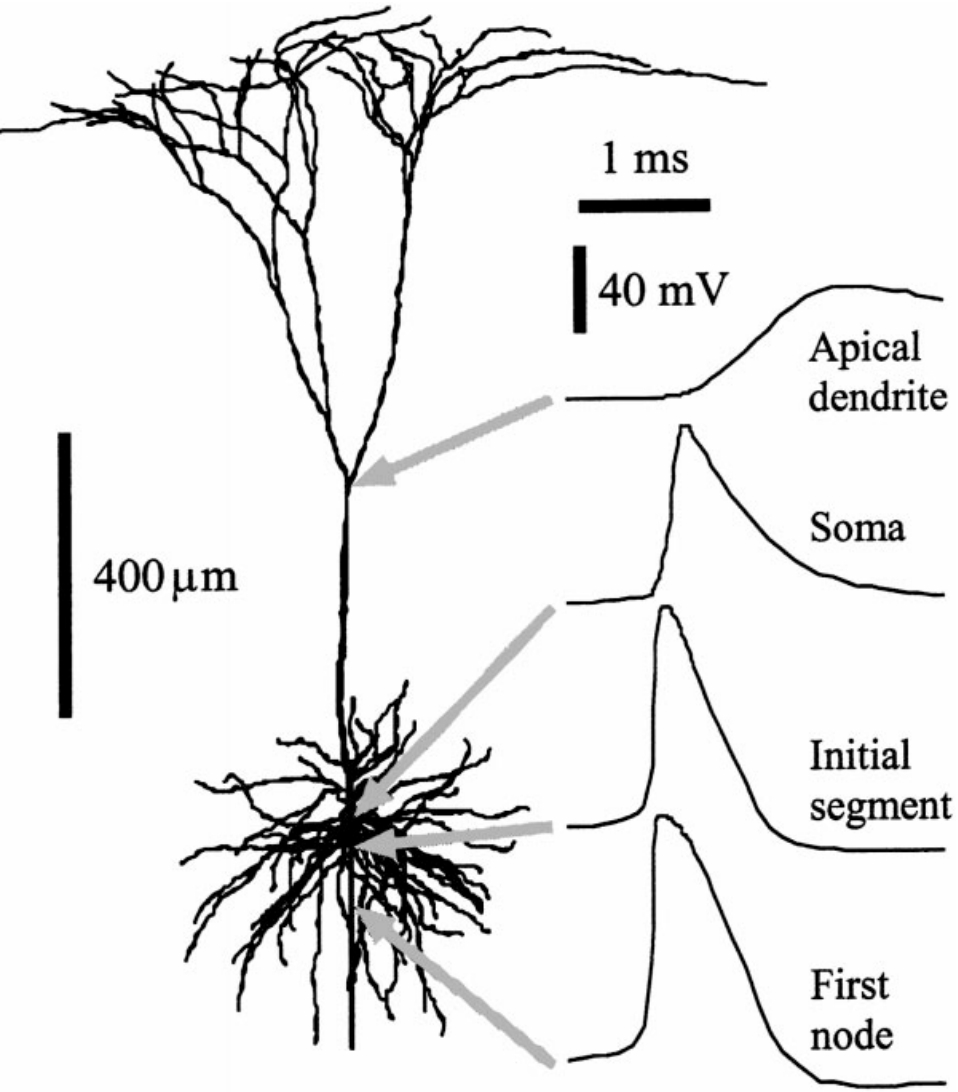
1 ms
40 mV
Apical dendrite
Soma
400 µm
Initial segment
First node

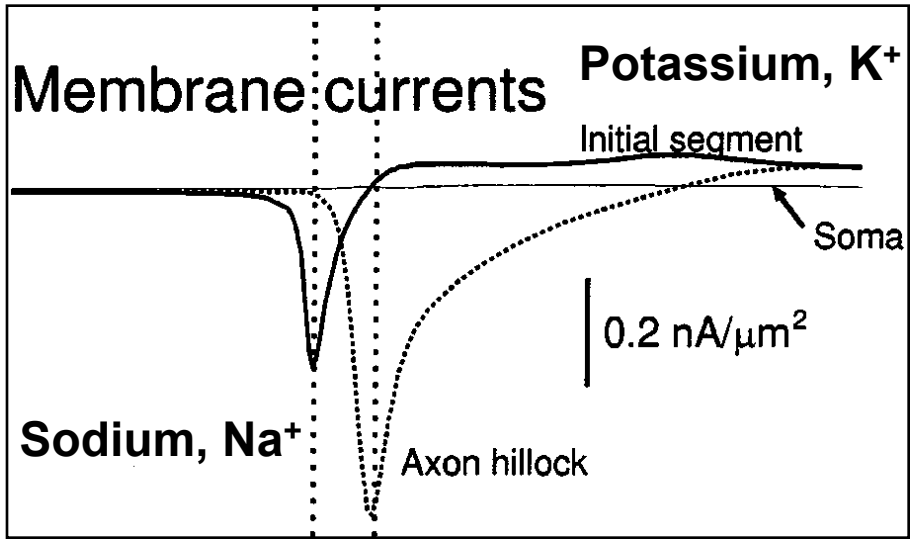
Membrane currents
Potassium, K+
Initial segment
Soma
0.2 nA/µm2
Sodium, Na+
Axon hillock

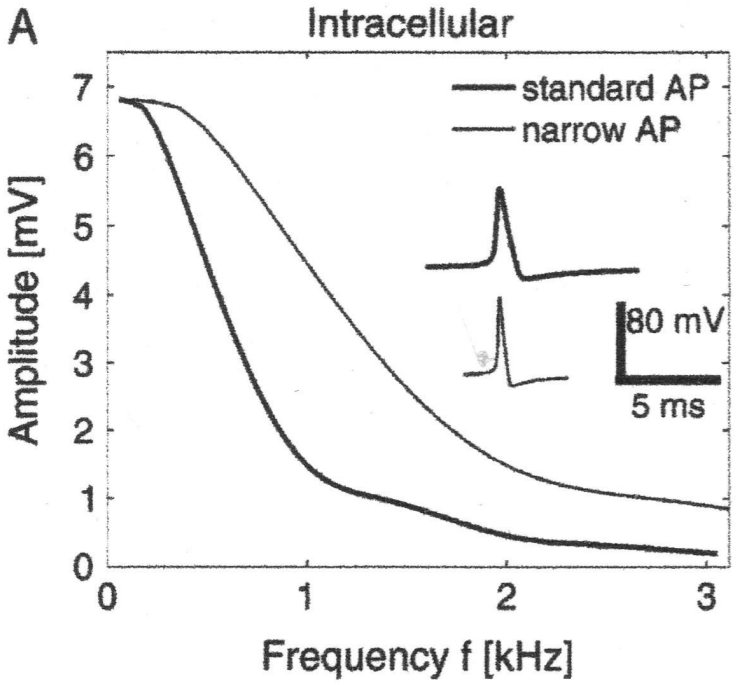
A
Intracellular
standard AP
narrow AP
80 mV
5 ms
Amplitude [mV]
Frequency f [kHz]
0
1
2
3
4
5
6
7

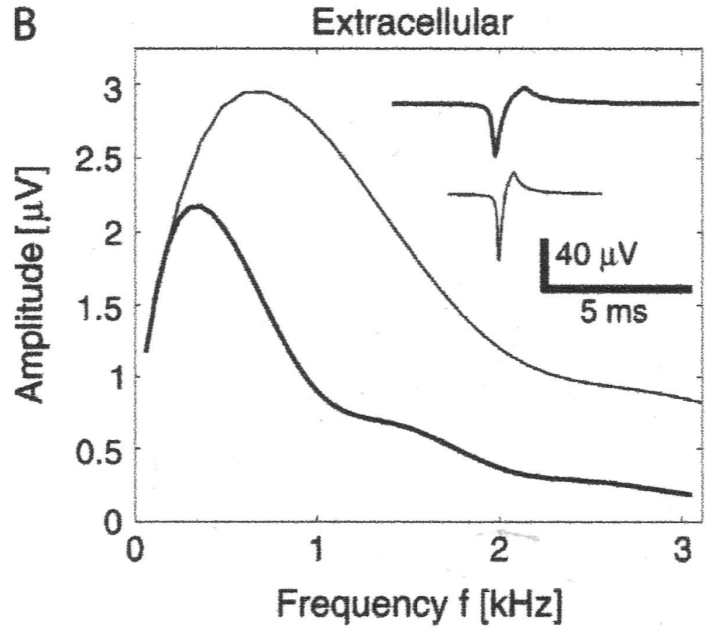
B
Extracellular
40 µV
5 ms
Amplitude [µV]
Frequency f [kHz]
0
0.5
1
1.5
2
2.5
3

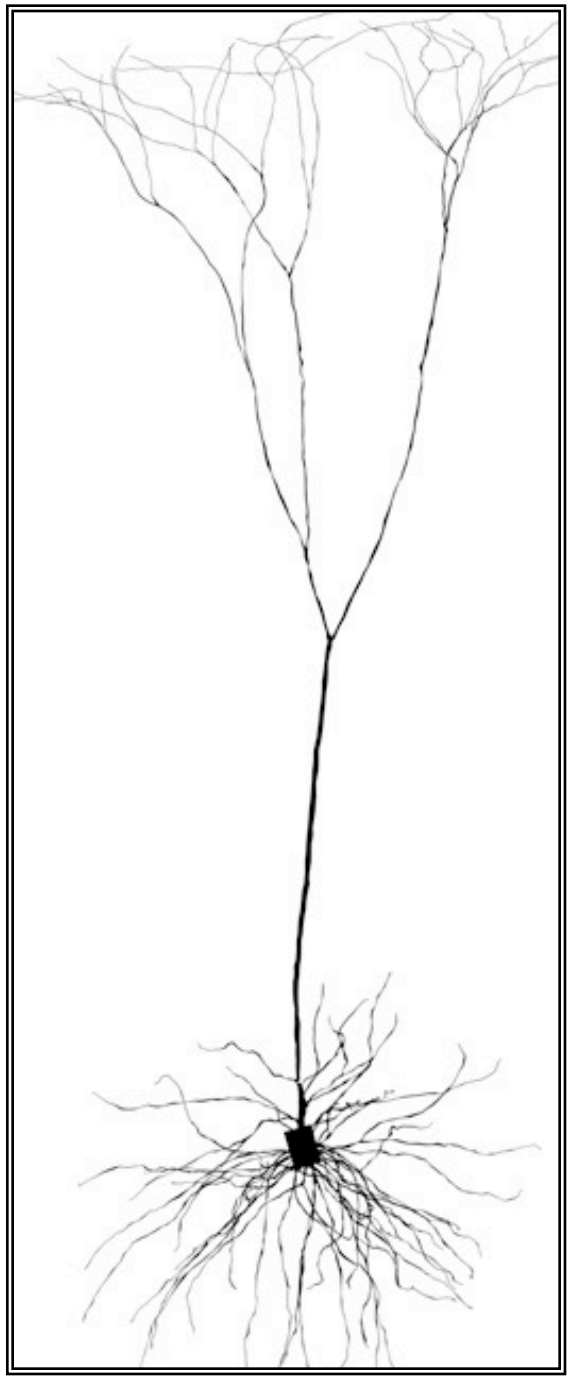

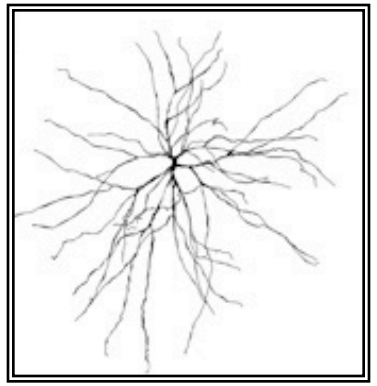

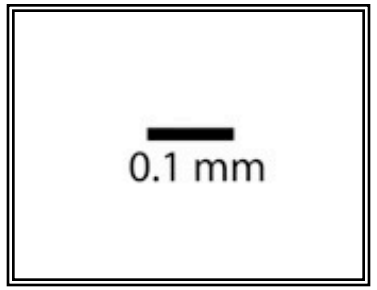
0.1 mm

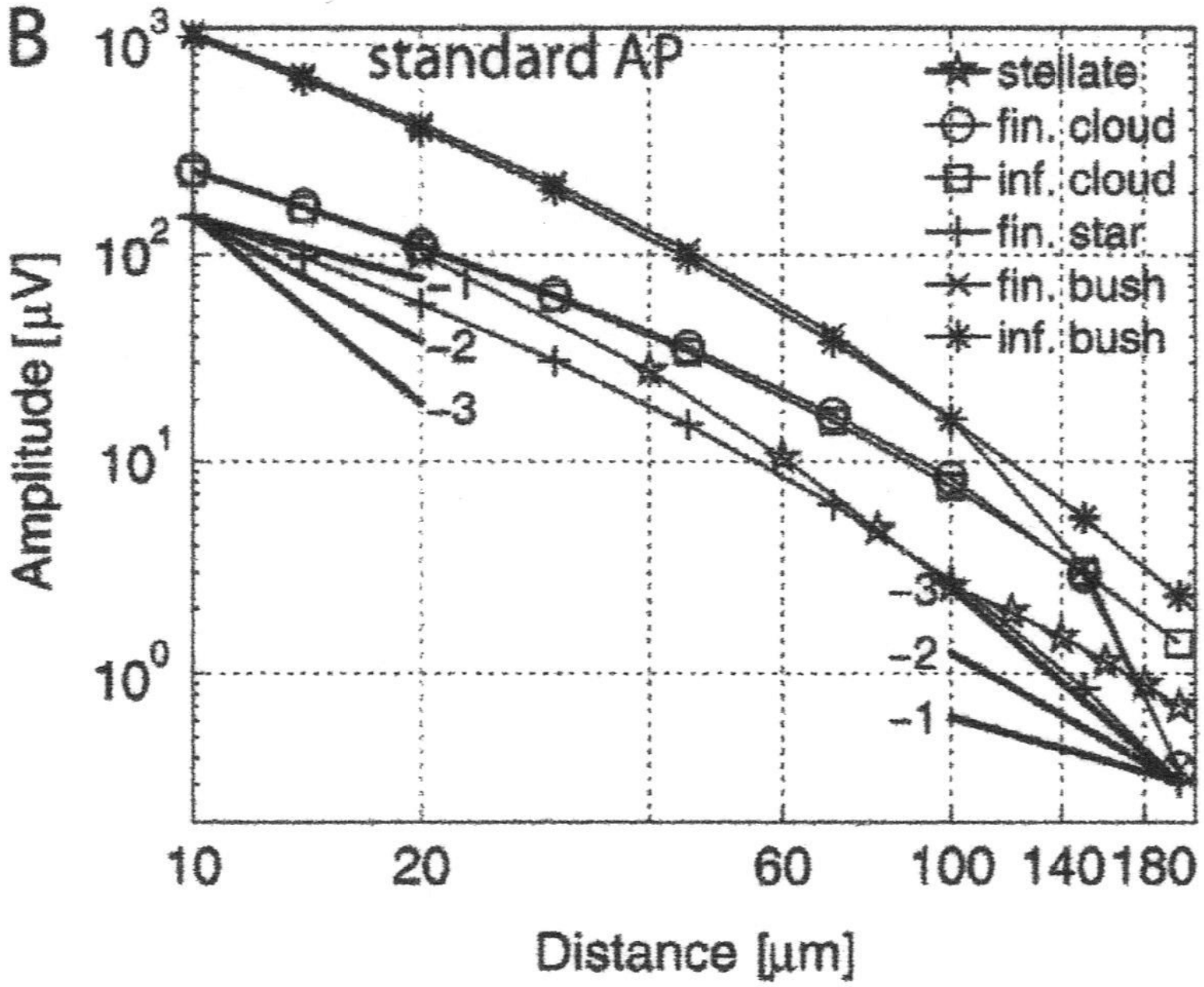

D

Amplitude [µV]

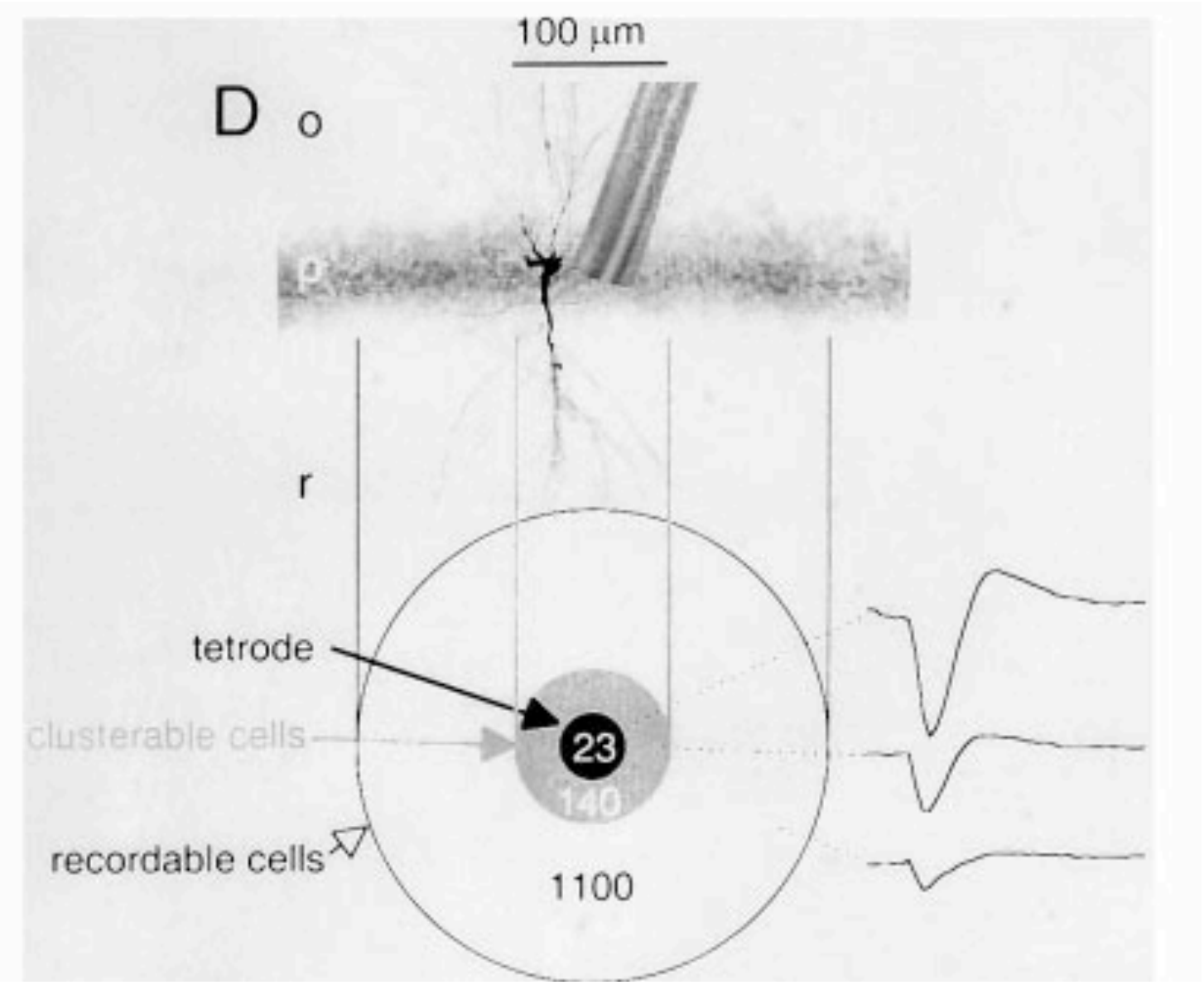
100 µm
D o
p
r
tetrode
clusterable cells
23
140
recordable cells
1100

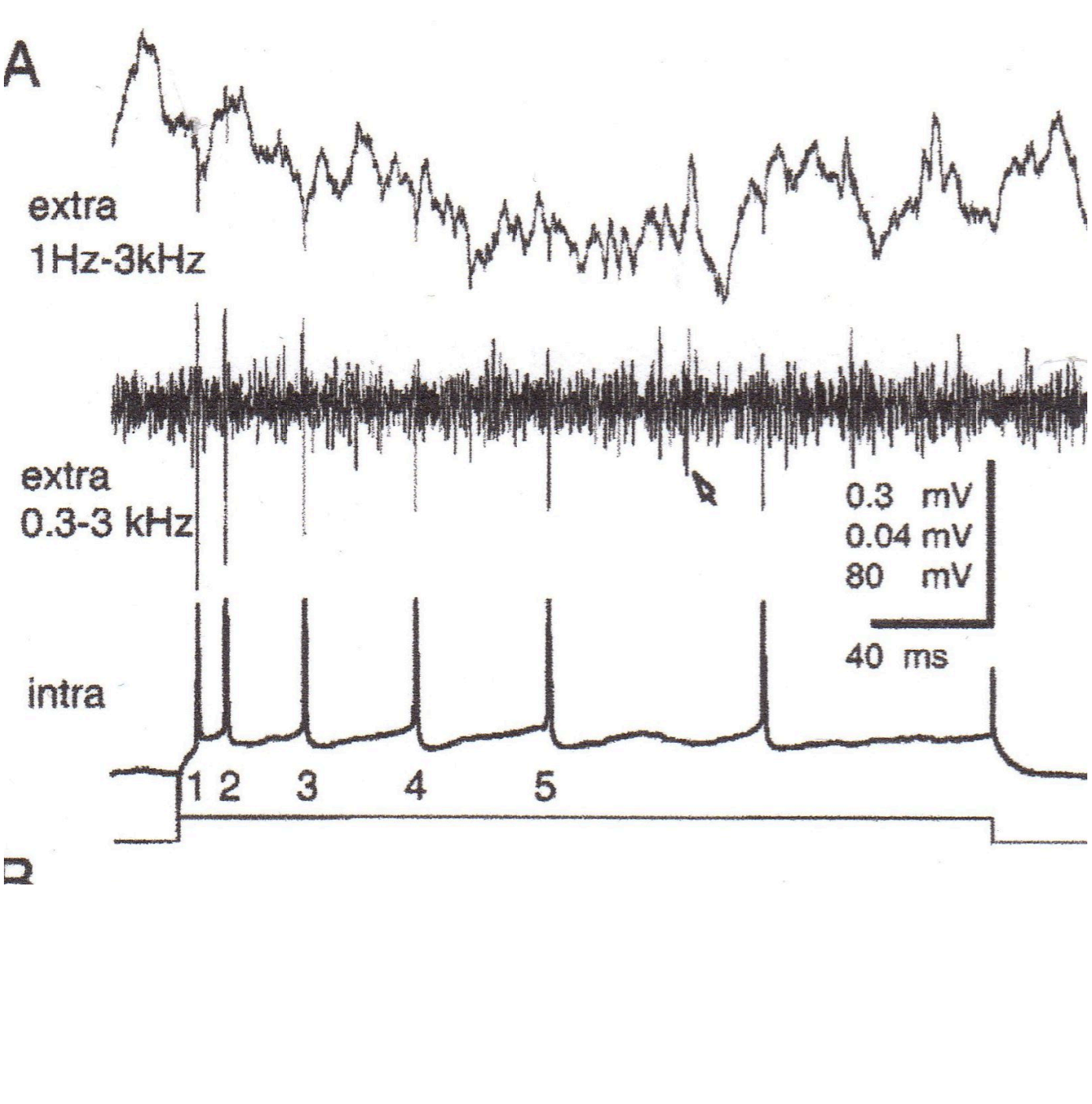
A
extra
1Hz-3kHz
extra
0.3-3 kHz
0.3 mV
0.04 mV
80 mV
40 ms
intra
1 2 3 4 5

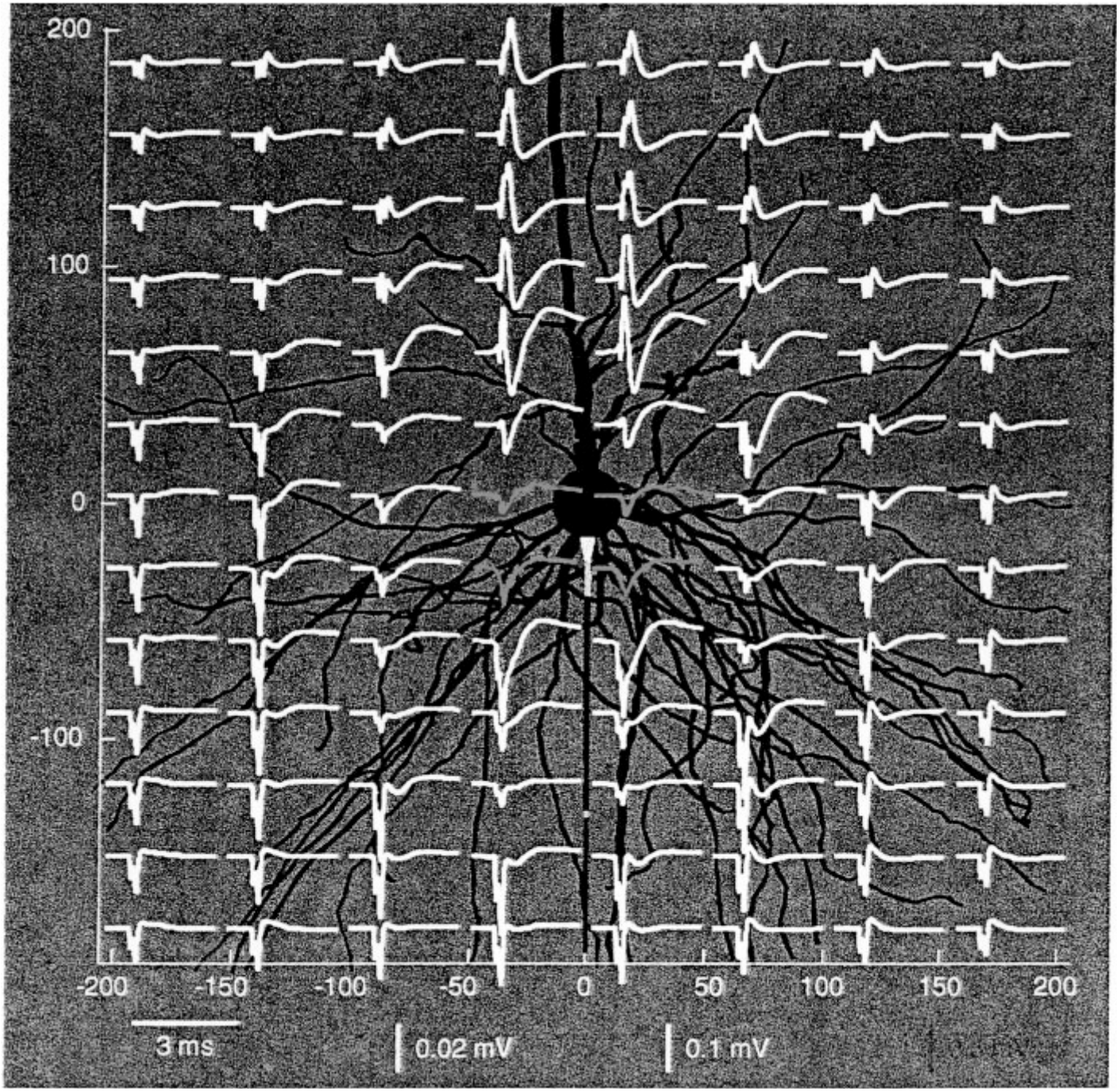
200
100
0
-100
-200
-150
-100
-50
0
50
100
150
200
3 ms
0.02 mV
0.1 mV

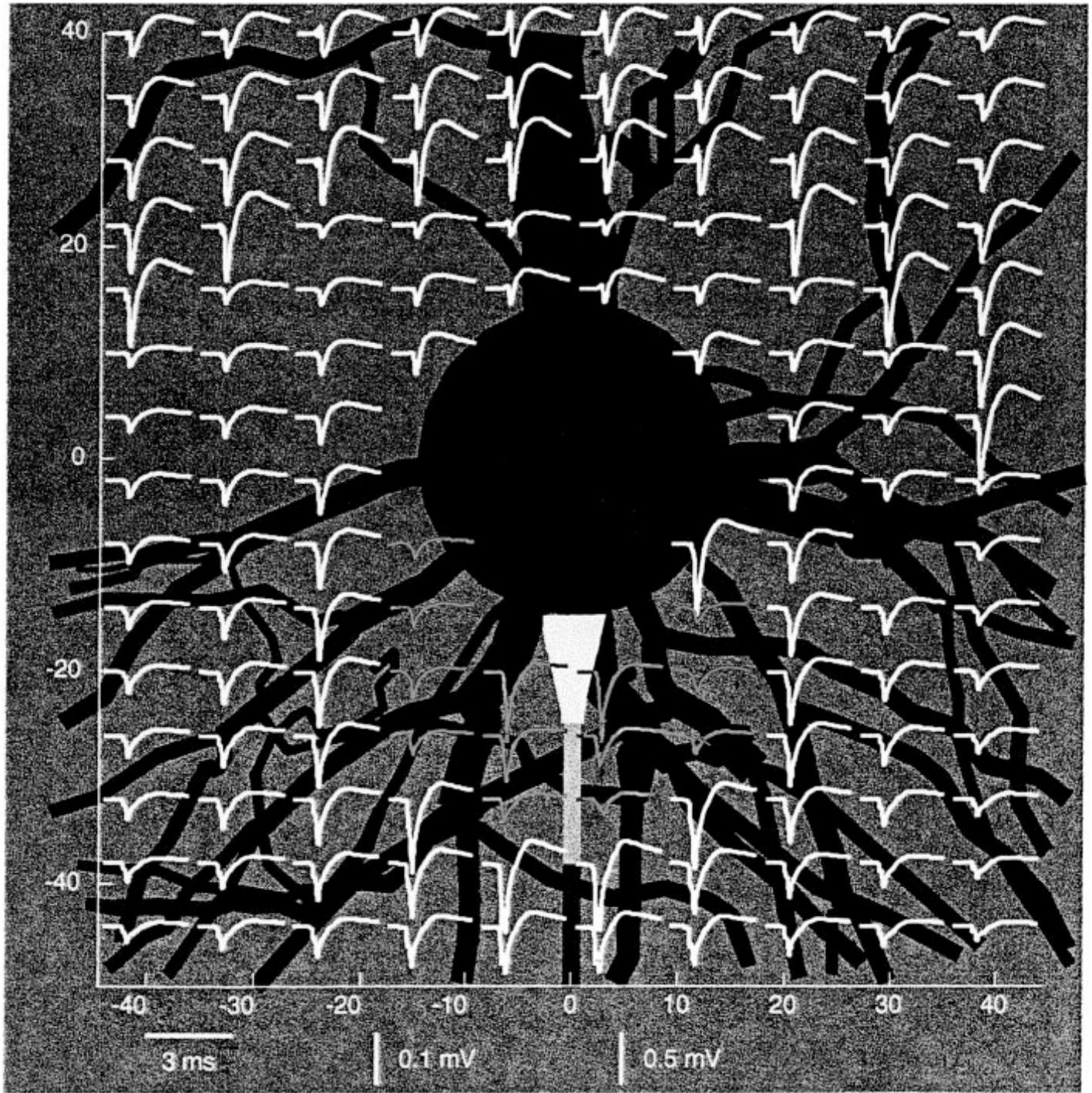
40
20
0
-20
-40
-40
-30
-20
-10
0
10
20
30
40
3 ms
0.1 mV
0.5 mV

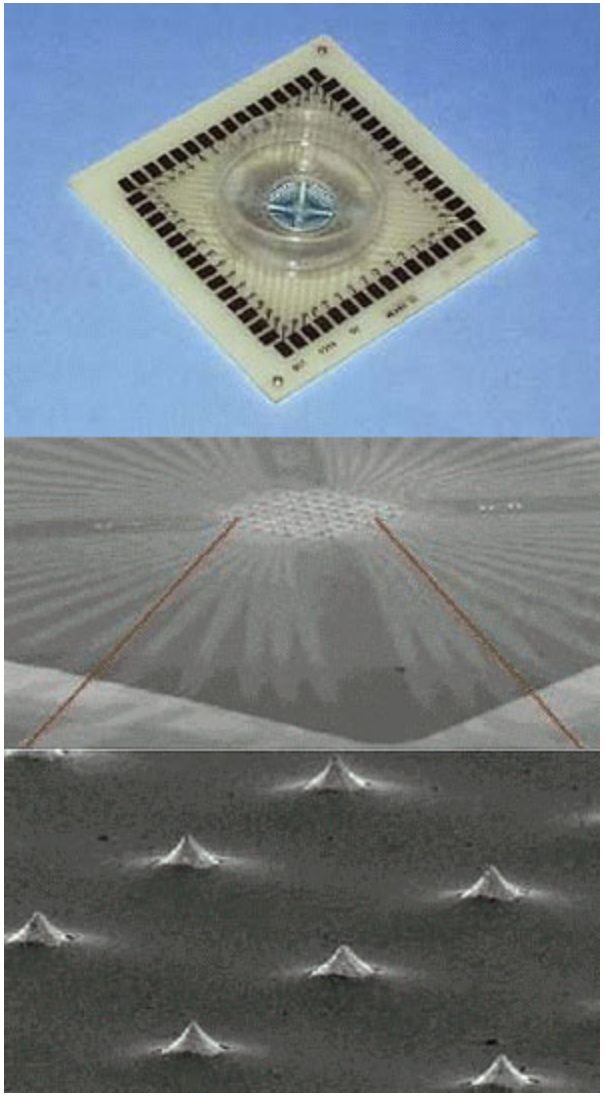

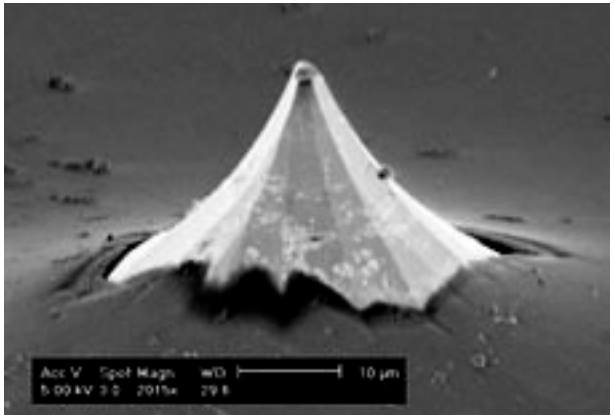

Next slide Mea 60 elettrodi, 3D amplitude > spike rate, burst duration 300 ms

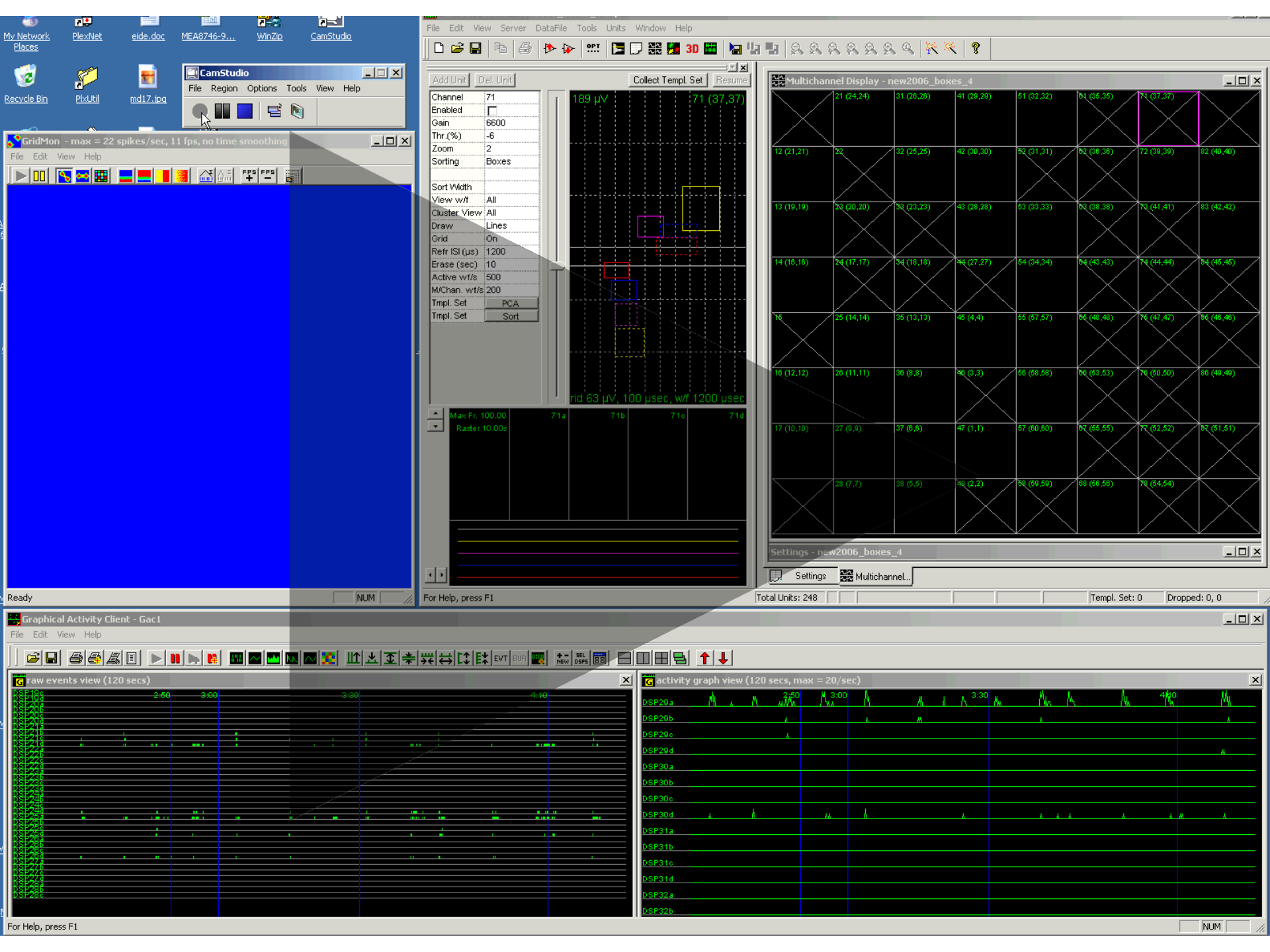
My Network Places
PlexNet
eide.doc
MEA8746-9...
WinZip
CamStudio
Recycle Bin
PlxUtil
md17.jpg
CamStudio
File Region Options Tools View Help
GridMon - max = 22 spikes/sec, 11 fps, no time smoothing
File Edit View Help
Ready
NUM
File Edit View Server DataFile Tools Units Window Help
Add Unit
Del. Unit
Collect Templ. Set
Resume
Channel 71
Enabled
Gain 6600
Thr.(%) -6
Zoom 2
Sorting Boxes
Sort Width
View w/f All
Cluster View All
Draw Lines
Grid On
Refr ISI (µs) 1200
Erase (sec) 10
Active wf/s 500
M/Chan. wf/s 200
Tmpl. Set PCA
Tmpl. Set Sort
189 µV
71 (37,37)
rid 63 µV, 100 µsec, w/f 1200 µsec
Max Fr. 100.00
Raster 10.00s
71a
71b
71c
71d
For Help, press F1
Multichannel Display - new2006_boxes_4
Settings - new2006_boxes_4
Settings
Multichannel...
Total Units: 248
Templ. Set: 0
Dropped: 0, 0
Graphical Activity Client - Gac1
File Edit View Help
raw events view (120 secs)
activity graph view (120 secs, max = 20/sec)
DSP29a
DSP29b
DSP29c
DSP29d
DSP30a
DSP30b
DSP30c
DSP30d
DSP31a
DSP31b
DSP31c
DSP31d
DSP32a
DSP32b
For Help, press F1
NUM

Multi-electrode array, MEA dishes

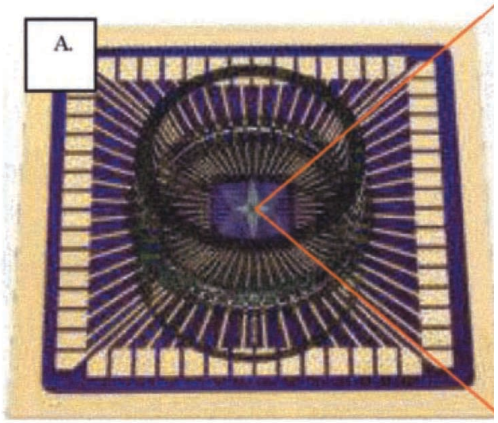

Organotypic slices

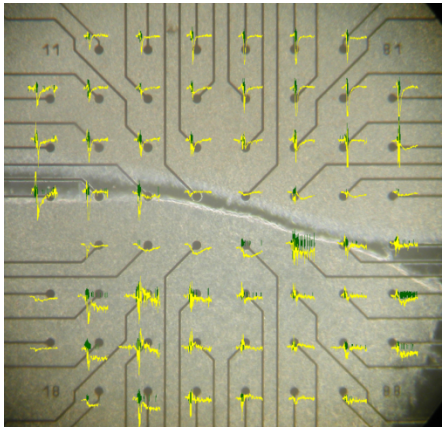

Recorded spikes and pharmacology

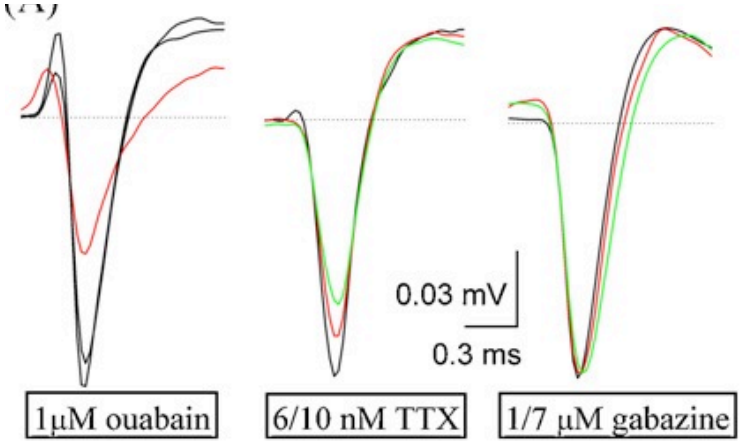

Neuron identification from a single electrode

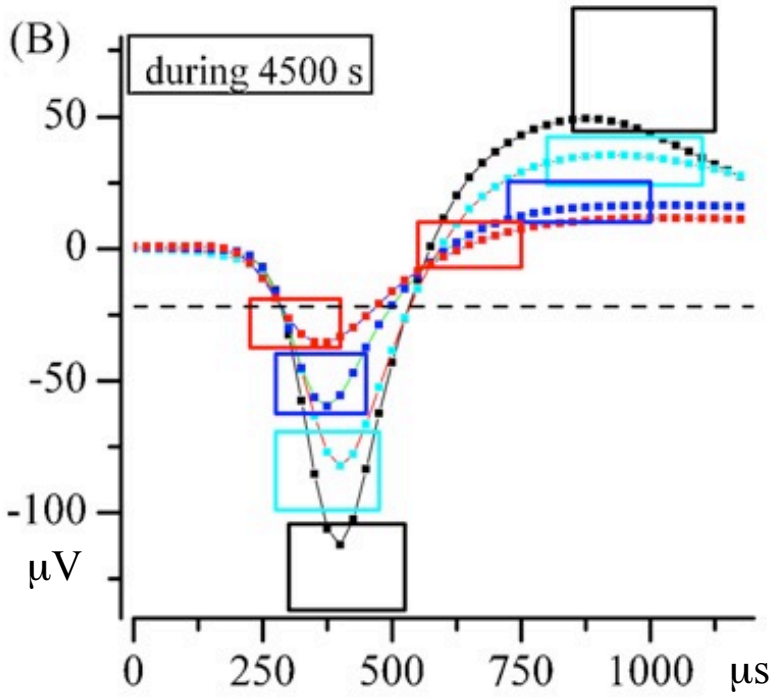

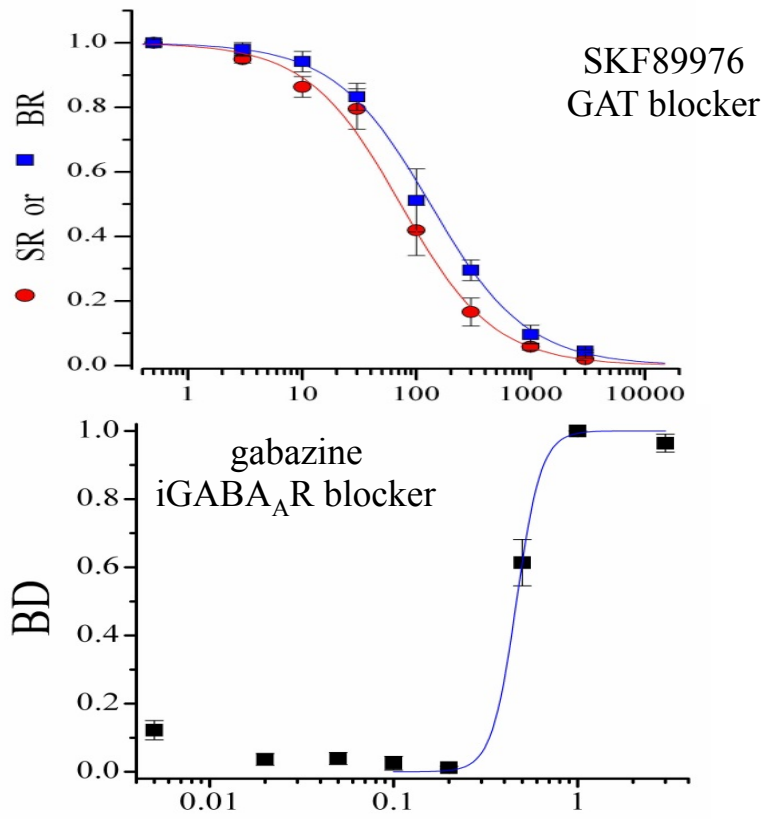

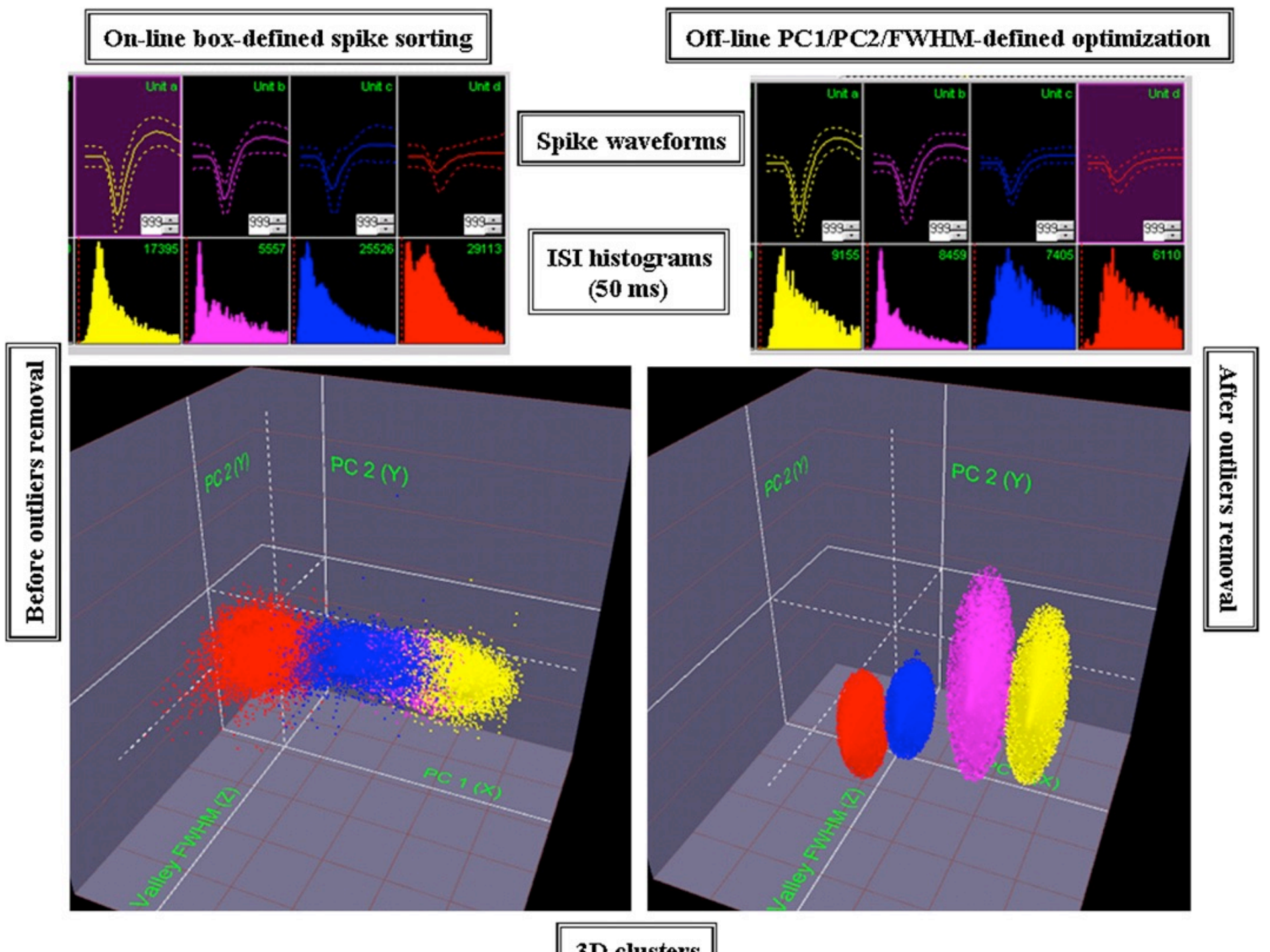
On-line box-defined spike sorting
Off-line PC1/PC2/FWHM-defined optimization
Unit a
Unit b
Unit c
Unit d
Spike waveforms
ISI histograms (50 ms)
17395
5557
25526
29113
9155
8459
7405
6110
Before outliers removal
After outliers removal
PC 2 (Y)
PC 1 (X)
Valley FWHM (Z)
3D clusters

Studies, in *in-vitro* networks of neurons, astrocytes and microglia, *19/49*

see: Sanchez-Vives & McCormick. Cellular and network mechanisms of rhythmic recurrent activity in neocortex. *Nat Neurosci* 2000, 3: 1027-34.

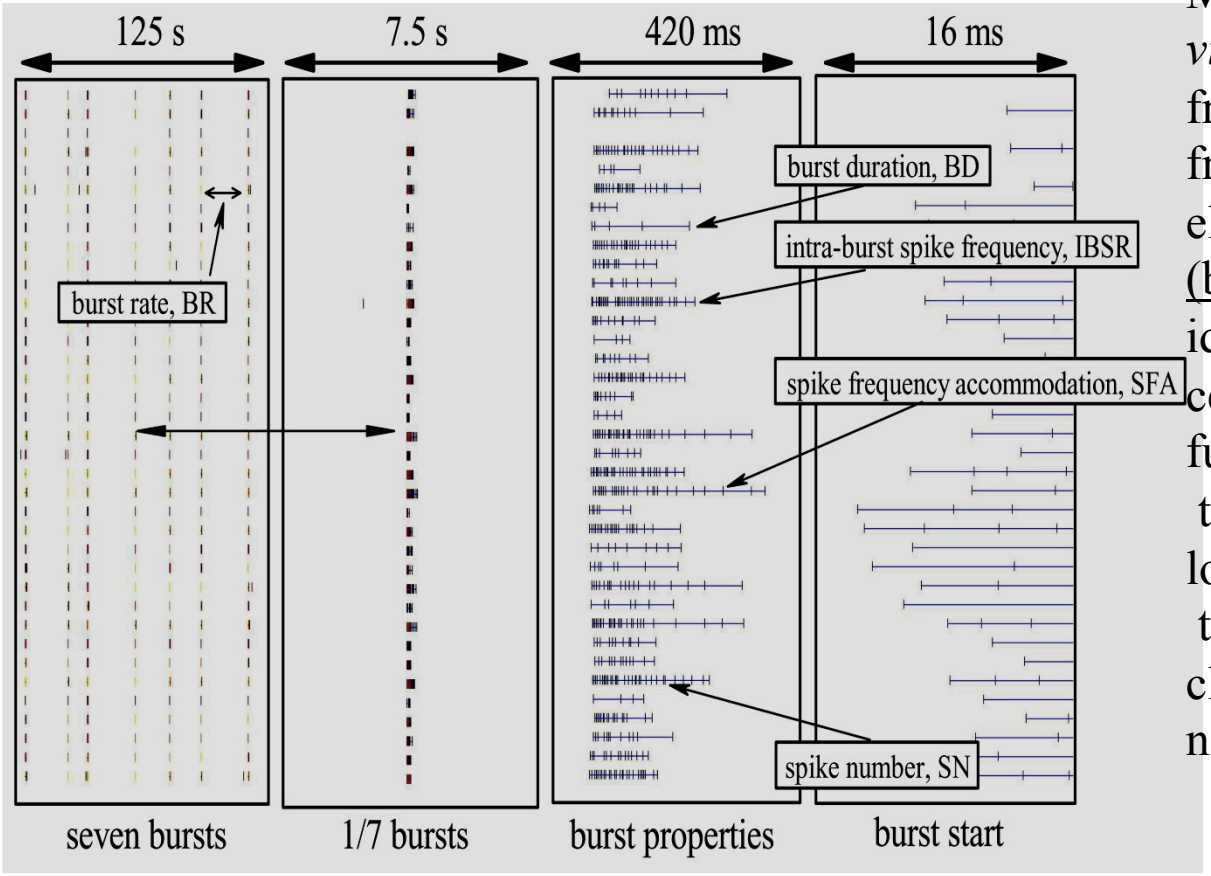

Methods: cultured networks of *ex-vivo* postnatal neocortex; activity from each network of 5,000 cells, from 60 electrodes by MEA electrophysiology; reverberating (bursts) activity was studied by identifying excitatory and inhibitory cells by their different autocorrelation function, ACF, computing the probability of finding short or long lasting burst durations (BD), the numbers of spikes elicited by clusters of excitatory and inhibitory neurons engaged in each burst.

Gullo F, Maffezzoli A, Dossi E, Wanke E. (2009) Short latency cross-and autocorrelation identify clusters of interacting neurons recorded from muti-electrode arrays. *J Neurosci Meth* 181:186-198.

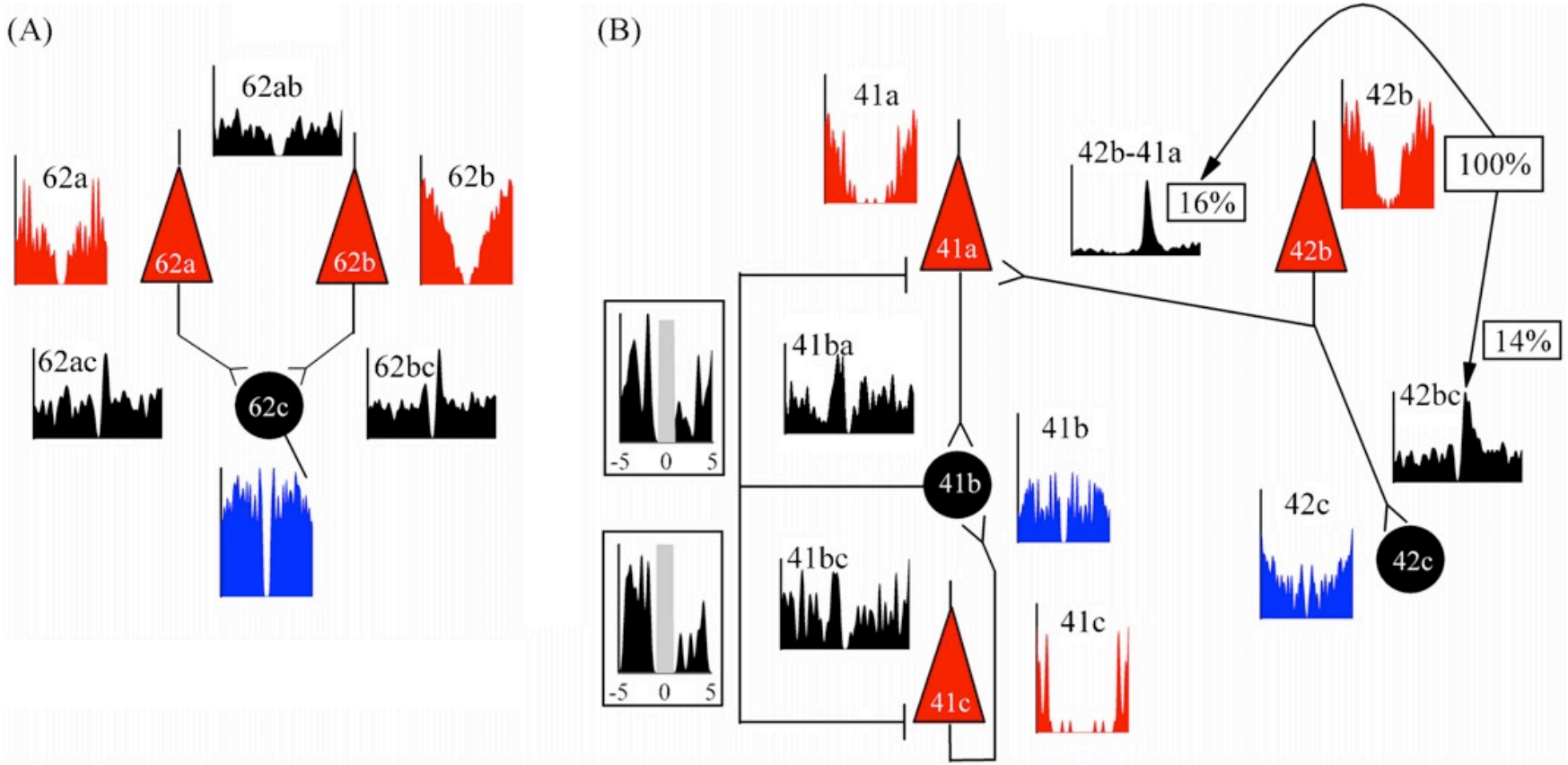

Short-latency analysis among units. The hypothesized wiring among putative neurons are derived from the data shown. Autocorrelogram, for **excitatory** or **inhibitory** cells and **crosscorrelograms** in black). Each plot has the same *x*-axis of ±20ms and the *y*-axis (spike/s) has values ranging from 8 to 20. (A) Units recorded from the same electrode in which only excitatory monosynaptic effects could be documented. (B) Data belong to two electrodes, 41 - 42 and to identified units of each one as indicated with letters. Insets show plots from −5 to +5ms and the shaded areas indicate the blank period of spike sampling during the on-line acquisition. Notice that autocorrelograms of excitatory and inhibitory cells are different. The 2 excitatory peaks (at 3.6 and 2.4 ms) shown in cross-correlograms to 41a and 42c correspond to 16 and 14% of the spikes of cell 42b, respectively (background activity was subtracted).

Gullo F, Maffezzoli A, Dossi E, Lecchi M, Wanke E. (2012) Classifying heterogeneity of spontaneous up-states: a method for revealing variations in firing probability, engaged neurons and Fano factor. *J Neurosci Methods* 203:407-17.

A

neuron-by-neuron strategy

Identification of **excitatory** and **inhibitory** neurons by autocorrelation analysis (Gullo et al., 2009)

Raster plot of timestamps: each *row* for *each* identified unit

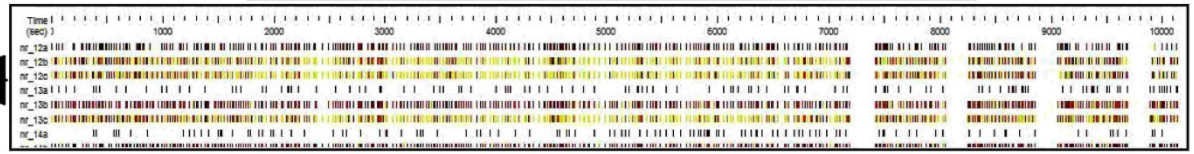

B1

burst-by-burst strategy

Network burst identification by a sliding window (bin-defined) (Ham et al., 2008; Gullo et al., 2010)

Raster plot of timestamps: *each* column for *each* burst

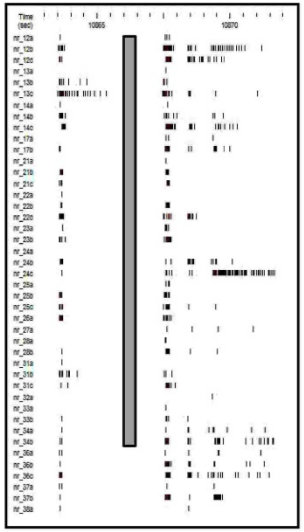

Novel Advanced Procedure

PCA-based K-Means classification of network states

Features: spike number time-histograms, neuron number, burst duration

B2

time-histograms of many states

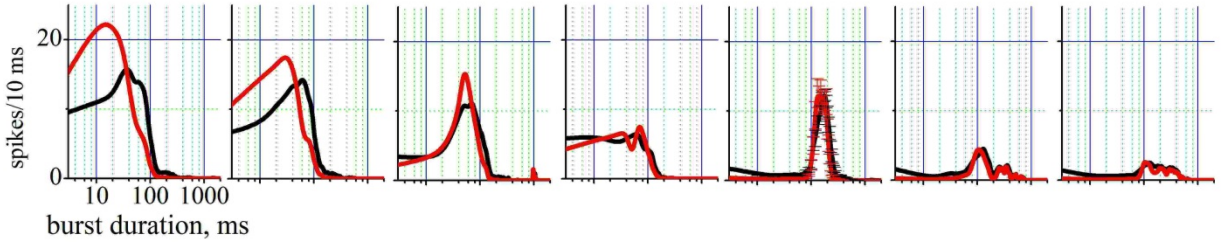

B3

for each state, cum. spike-histograms, time-histogram of neuron number and Fano factor

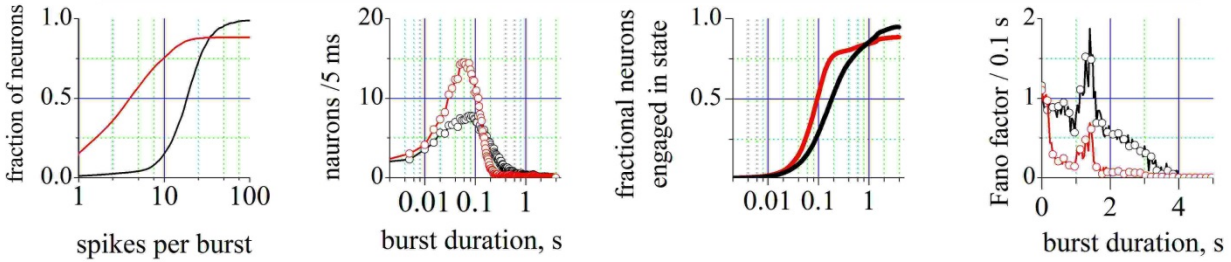

Fig.1

ACF versus FF sorting

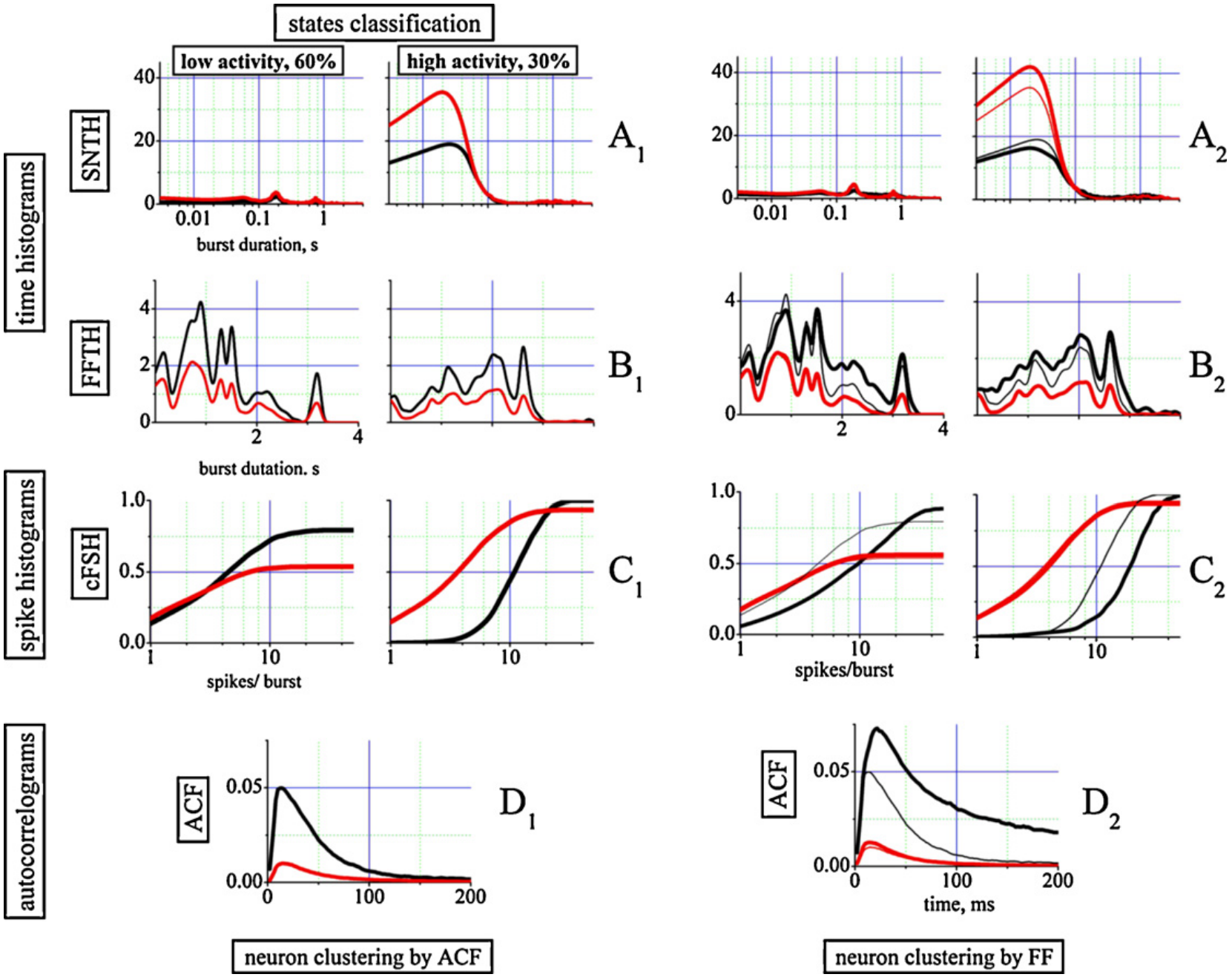

Identification of neurons by using a knock-in mice expressing a fluorescent protein (GFP) only in GABAergic neurons

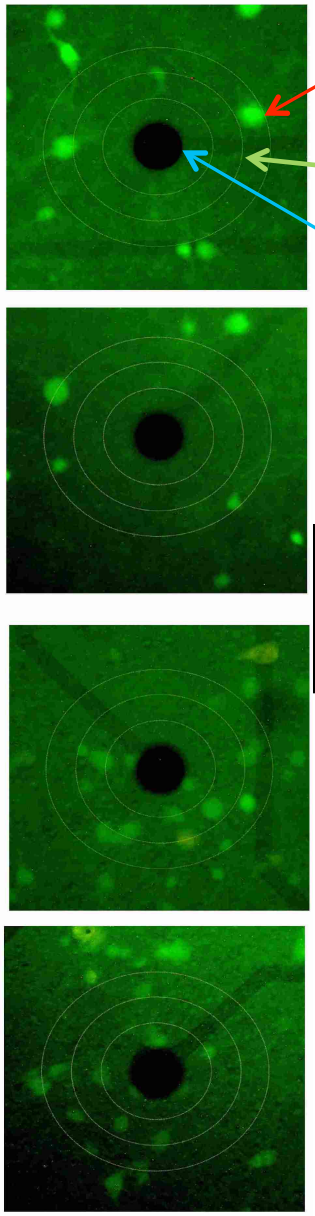

excitatory neurons are not fluorescent and almost *invisible*

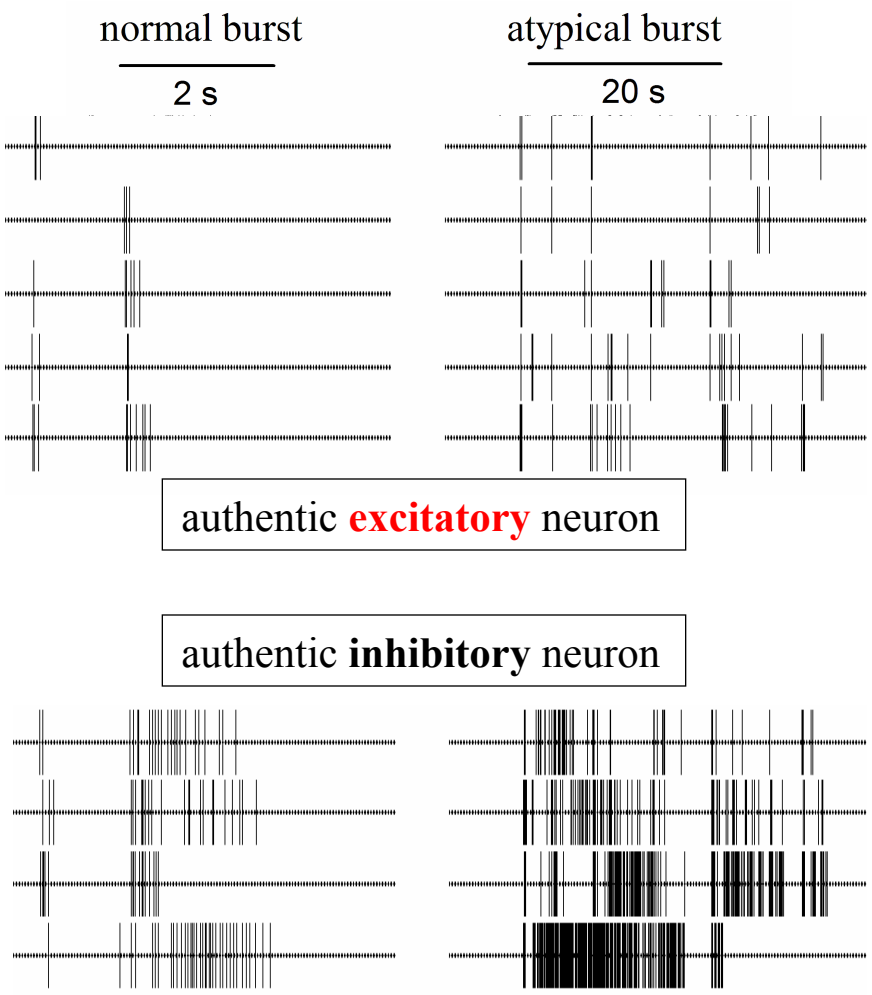

Becchetti A, Gullo F, Bruno G, Dossi E, Lecchi M and Wanke E. (2012) Exact distinction of excitatory and inhibitory neurons in neural networks: a study with GFP-GAD67 neurons optically and electrophysiologically recognized on multielectrode arrays. *Front. Neural Circuits 6:63*. doi: 10.3389/fncir.2012.00063.

Neuron-glia crosstalk revealed in reverberating networks by simultaneous extracellular recording of spikes and astrocytes' glutamate transporter and K^+ currents. *25-51*

by

Wanke E, Gullo F, Dossi E, Valenza G[1], Becchetti A.

Department of Biotechnologies and Biosciences and

Milan Center For Neuroscience (NeuroMI), University of Milano-Bicocca, Milan, Italy

[1]Research Centre "E. Piaggio" and Department of Information Engineering, School of Engineering, University of Pisa, Pisa, Italy - *J Neurophysiol. 28:2706-2719, 2016*

Other CNS cells crucially supporting neuronal activity: astrocytes control the concentration of potassium (K^+) and glutamate (the excitatory neurotransmitter) by an ion channel and a neurotransporter (GluT)

Viewing the whole network from one electrode

Filtering strategy: distortions and signal reconstruction by deconvolution

Slow signals, power spectra for K^+ currents and killing astrocytes during growing

The response of an astrocyte to a single spike

The network become epileptic if GluT is blocked

The different responses of adjacent astrocytes

The future: simulate microglial cells controlling CNS neuroinflammation

Glutamate transporter restores $[glu]_o$

Inward current removes the firing-induced increase of $[K^+]_o$

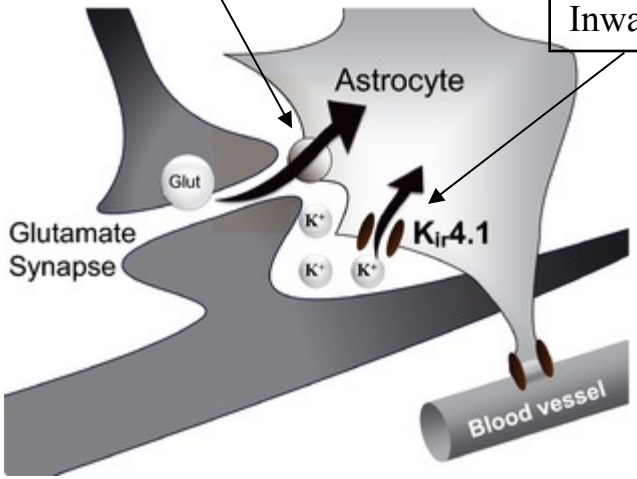

In CNS networks about 50% of the cells are neurons and 50% are glial cells subdivided into 40% astrocytes and 10% microglial cells, activated during inflammation.

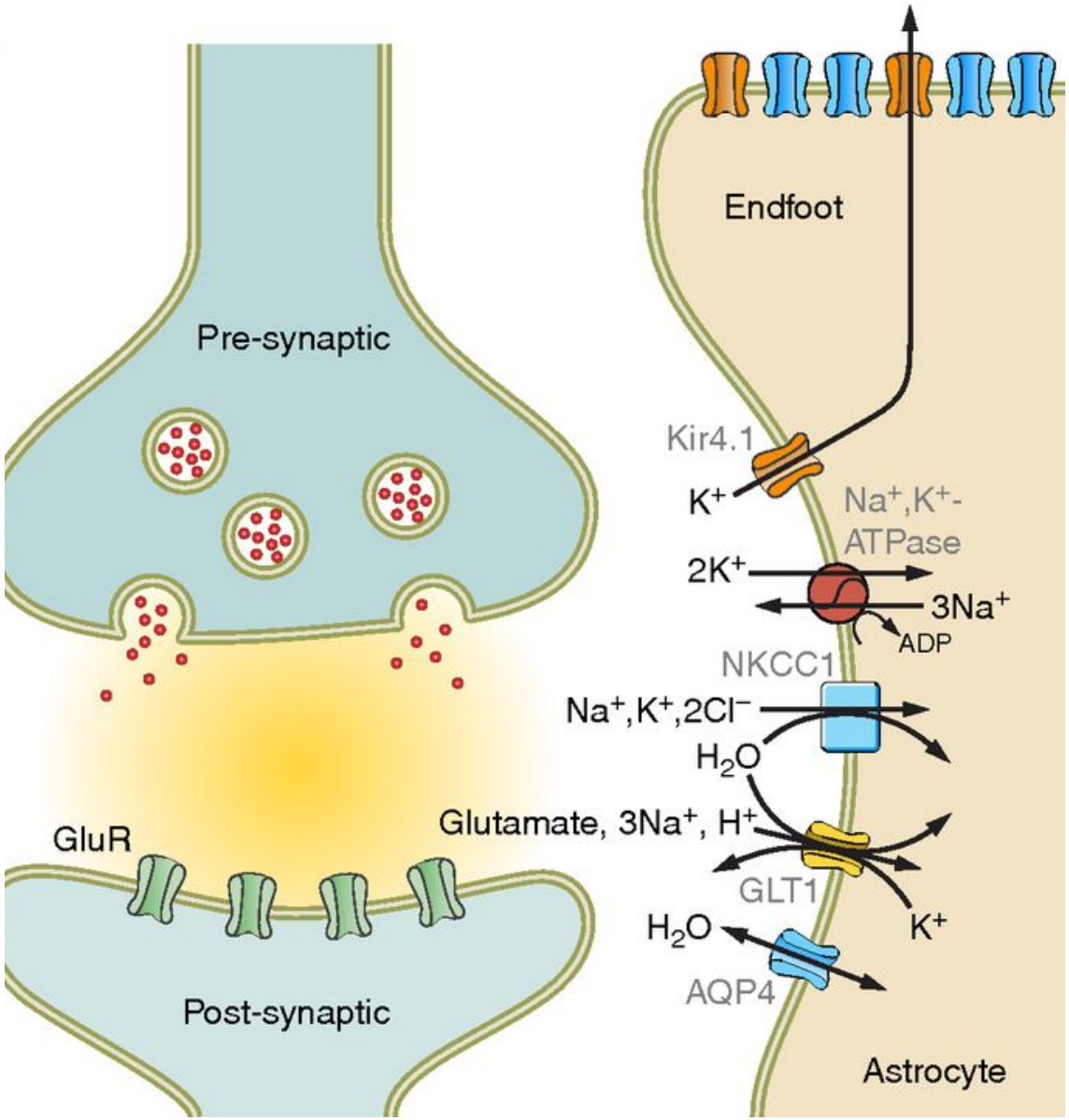

Amzica, Florin and Dag Neckelmann. Membrane capacitance of cortical neurons and glia during sleep oscillations and spike-wave seizures. *J. Neurophysiol.* 82: 2731–2746, 1999. Dual intracellular recordings in vivo were used to disclose relationships between cortical

Each spike causes an increase of $[K^+]_o$

Spikes from neurons

Membrane potential of neurons at resting -65 mV

Membrane potential of astrocytes -90 mV

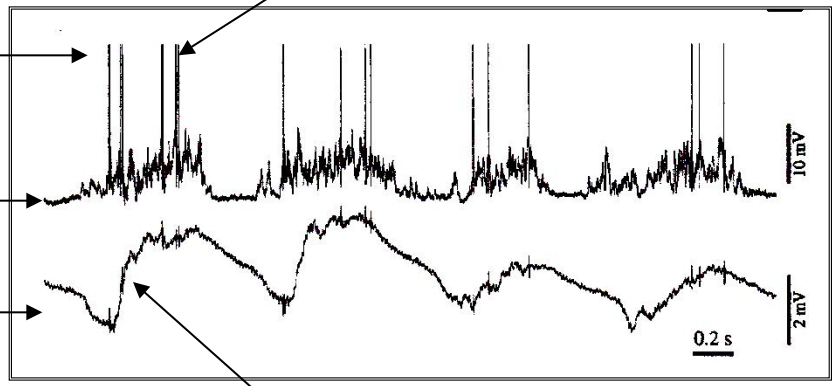

slow $[K^+]_o$ -induced depolarization, see below

R. K. ORKAND,[2] J. G. NICHOLLS,[3] AND S. W. KUFFLER
Neurophysiology Laboratory, Department of Pharmacology, Harvard Medical School, Boston, Massachusetts

(Received for publication February 7, 1966)

EFFECT OF NERVE IMPULSES ON THE MEMBRANE POTENTIAL OF GLIAL CELLS IN THE CENTRAL NERVOUS SYSTEM OF AMPHIBIA[1]

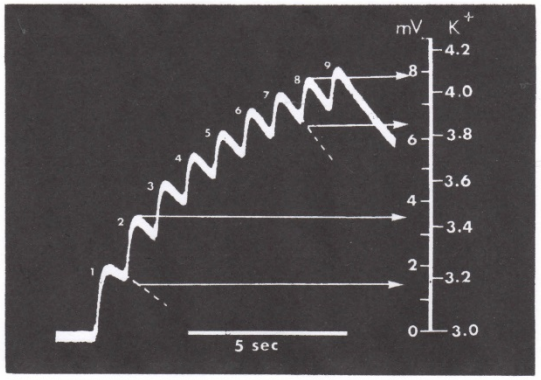

FIG. 6. Record of nine successive glial depolarizations set up by maximal nerve volleys at 1-sec. intervals. Extrapolation of the falling phase of the first and seventh depolarization shown by a dashed line. The depolarization is given in millivolts on the left side of the scale. On the right side are given the values of external K^+ concentrations in mEq/liter which would produce equivalent depolarizations (calculated from the Nernst equation). The second depolarization with an amplitude of 2.04 mV. is equivalent to the addition of 0.26 mEq/liter K^+ (distance on scales between lower two arrows). The eighth depolarization, 1.52 mV., is equivalent to the addition of 0.25 mEq/liter K^+ (upper two arrows, see Table 2).

Remember this panel

P. Kofuji and E. A. Newman / Neuroscience 129 (2004) 1045–1056

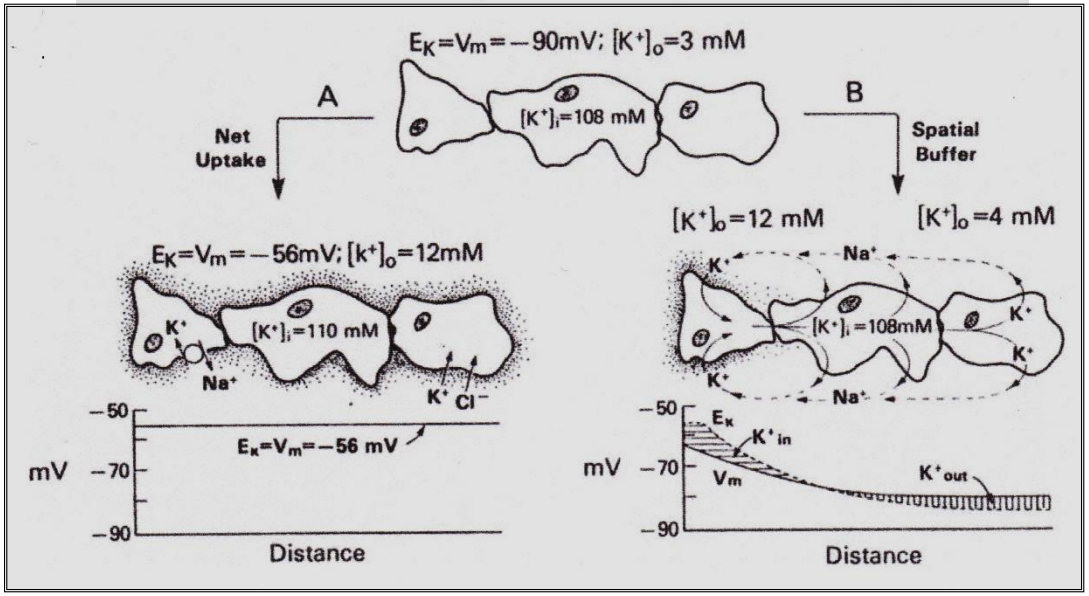

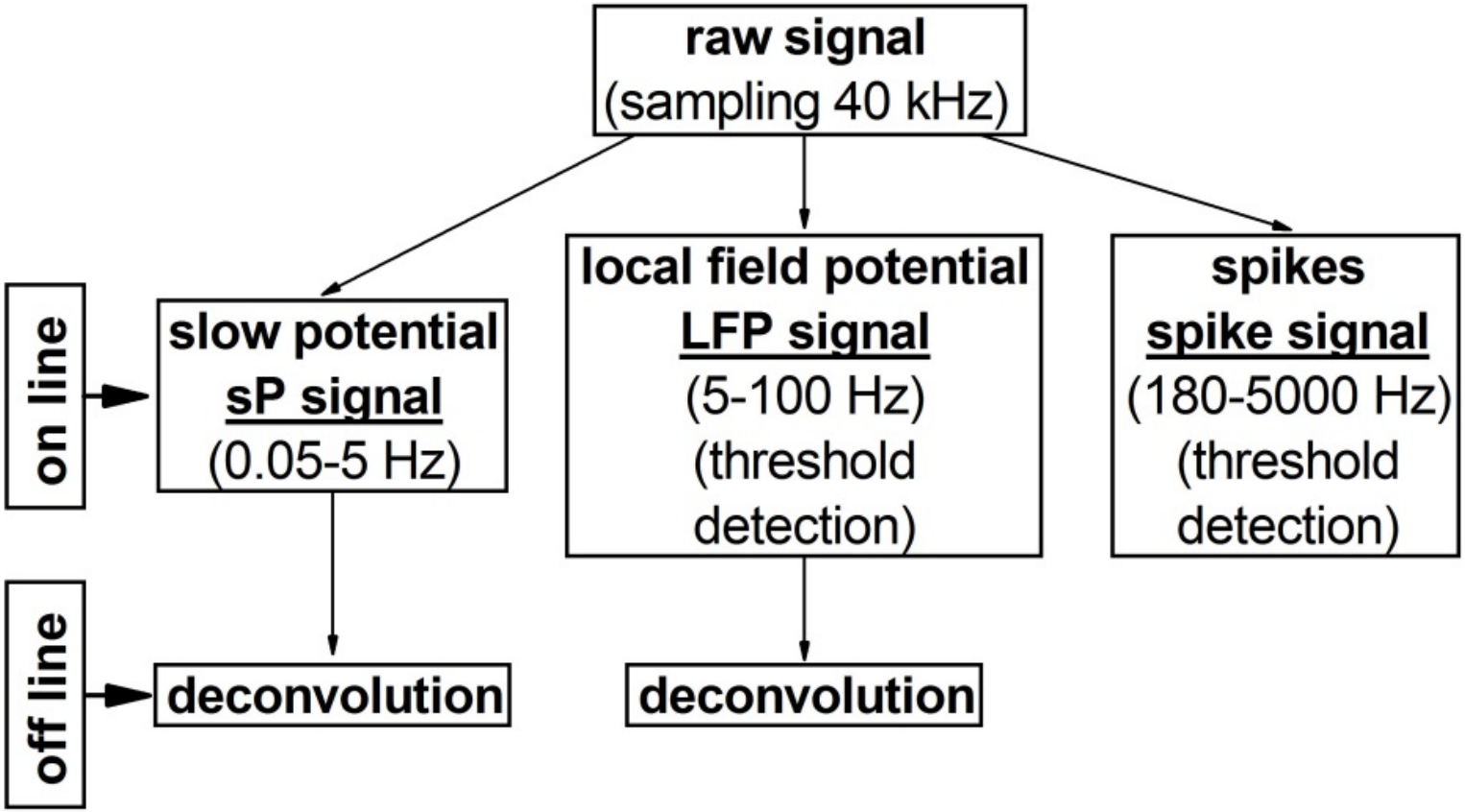

Given the acquired time dependent signals $Y_{sP}(t)$ and $Y_{LFP}(t)$ and the actual impulse responses $H_{sP}(t)$ and $H_{LFP}(t)$ of the filters used to acquire, respectively, sP and LFP signals (*Fig*. 1, *B2* and *B3*), the estimated inputs $X_{sP}(t)$ and $X_{LFP}(t)$ are respectively defined as

$$X_{sP}(t) = iFFT[X_{sP}(f)] = iFFT[Y_{sP}(f) / H_{sP}(f)] \quad (1)$$

and

$$X_{LFP}(t) = iFFT[X_{LFP}(f)] = iFFT[Y_{LFP}(f) / H_{LFP}(f)] , \quad (2)$$

where iFFT is the inverse fast Fourier transform and $X_{sP}(f)$, $Y_{sP}(f)$, $H_{sP}(f)$, $X_{LFP}(f)$, $Y_{LFP}(f)$, and $H_{LFP}(f)$ refer to Fourier transform representations
in the frequency domain.

Impulse responses of the three filters

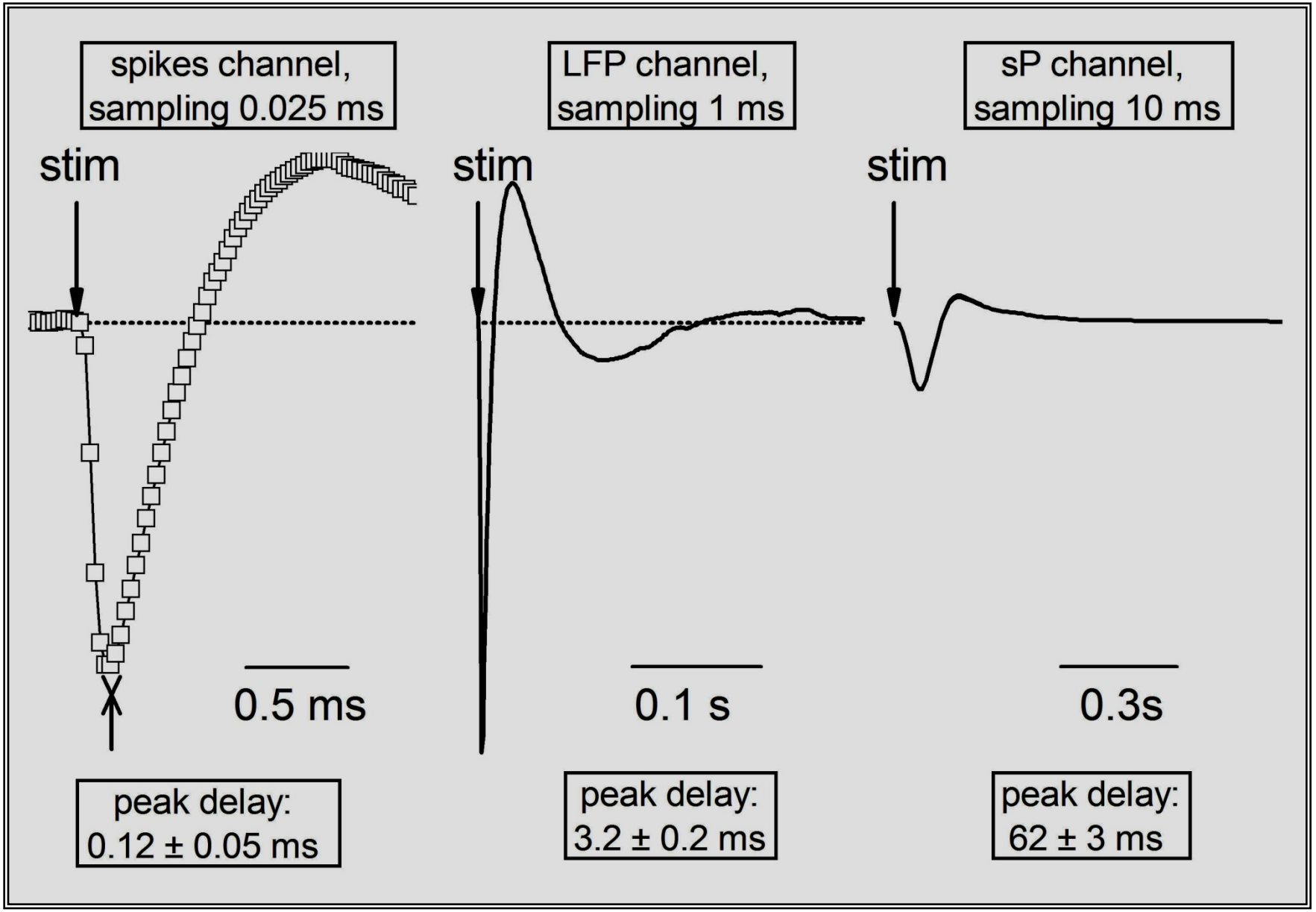

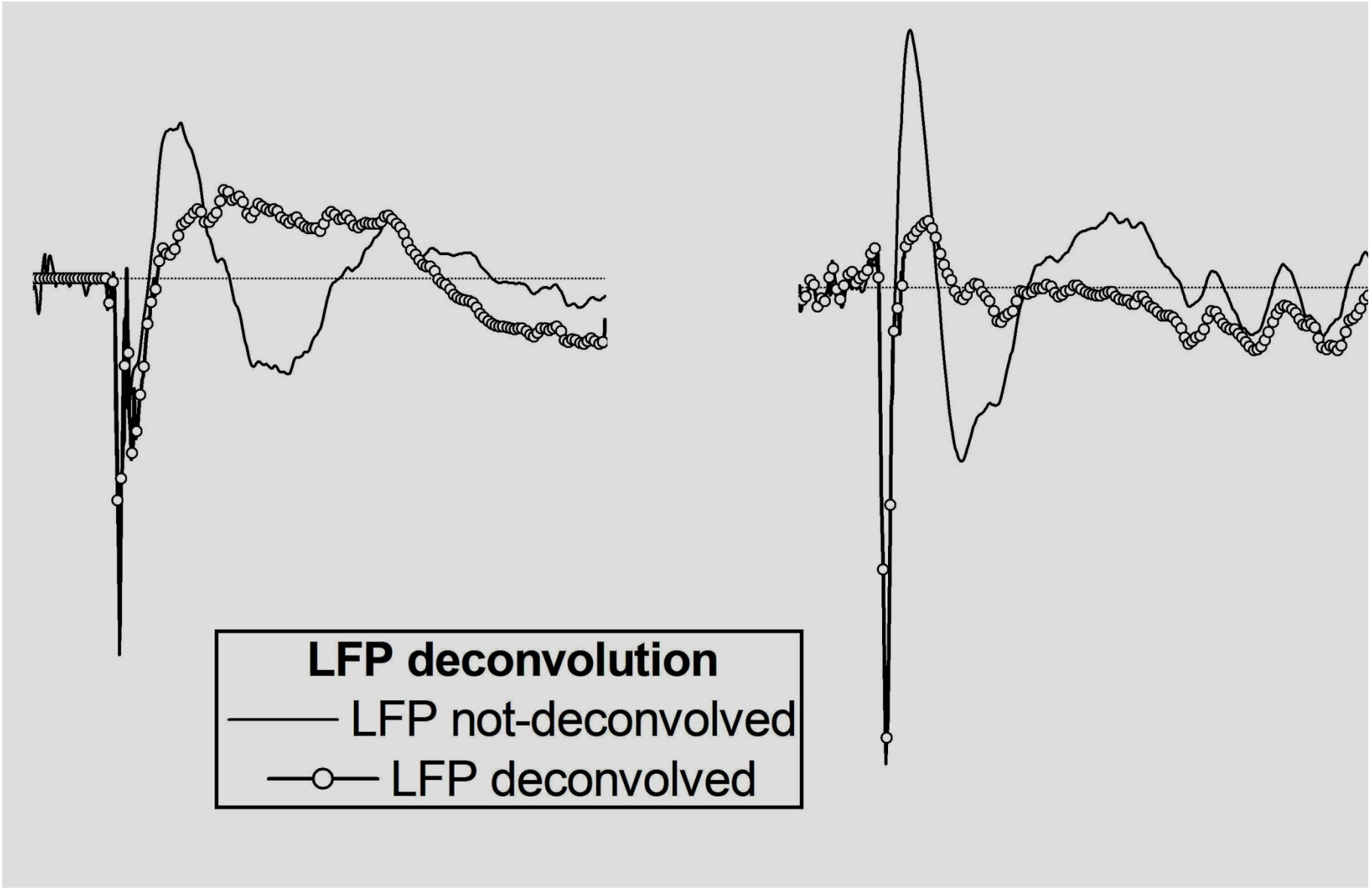
LFP deconvolution
LFP not-deconvolved
LFP deconvolved

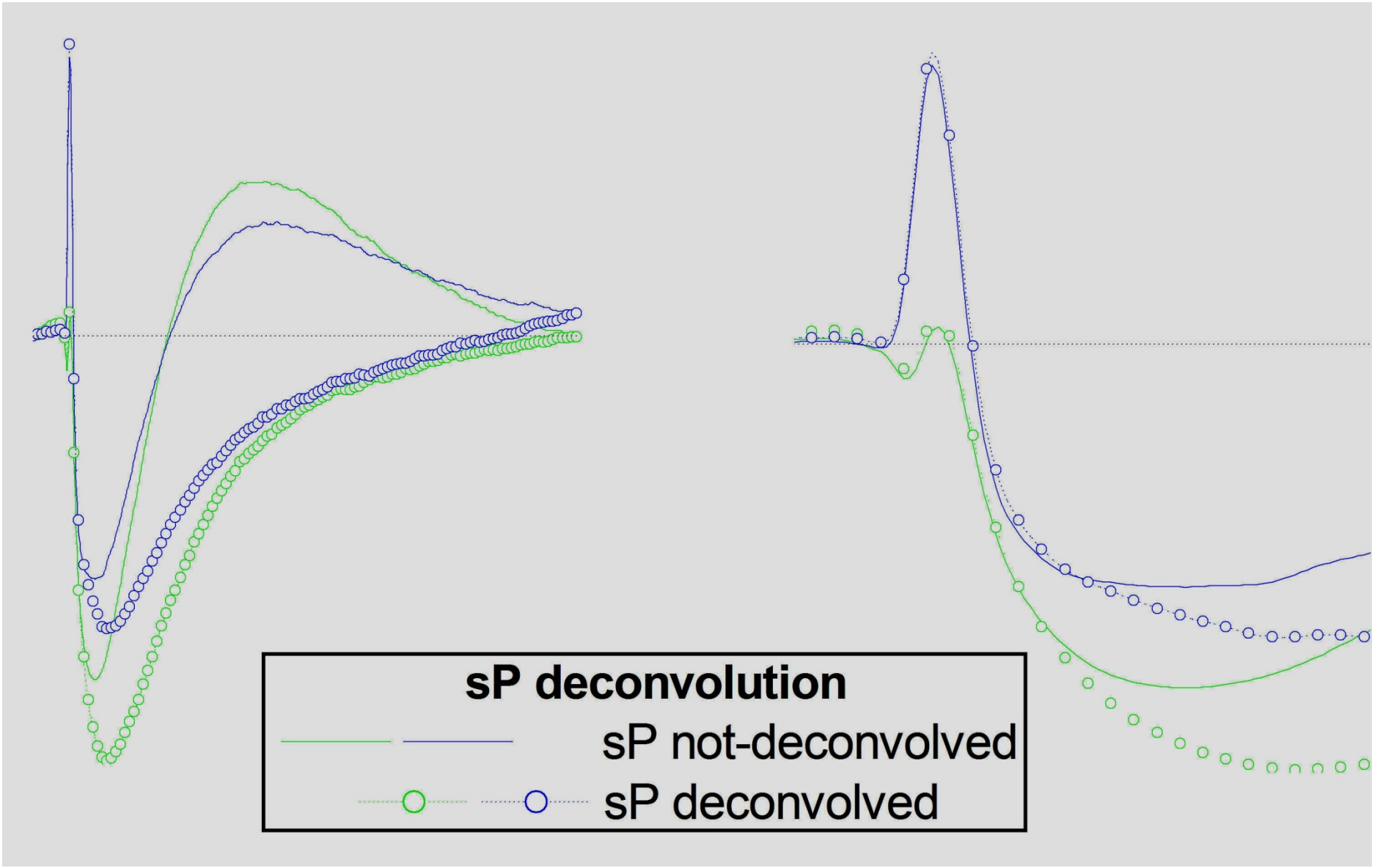
sP deconvolution
sP not-deconvolved
sP deconvolved

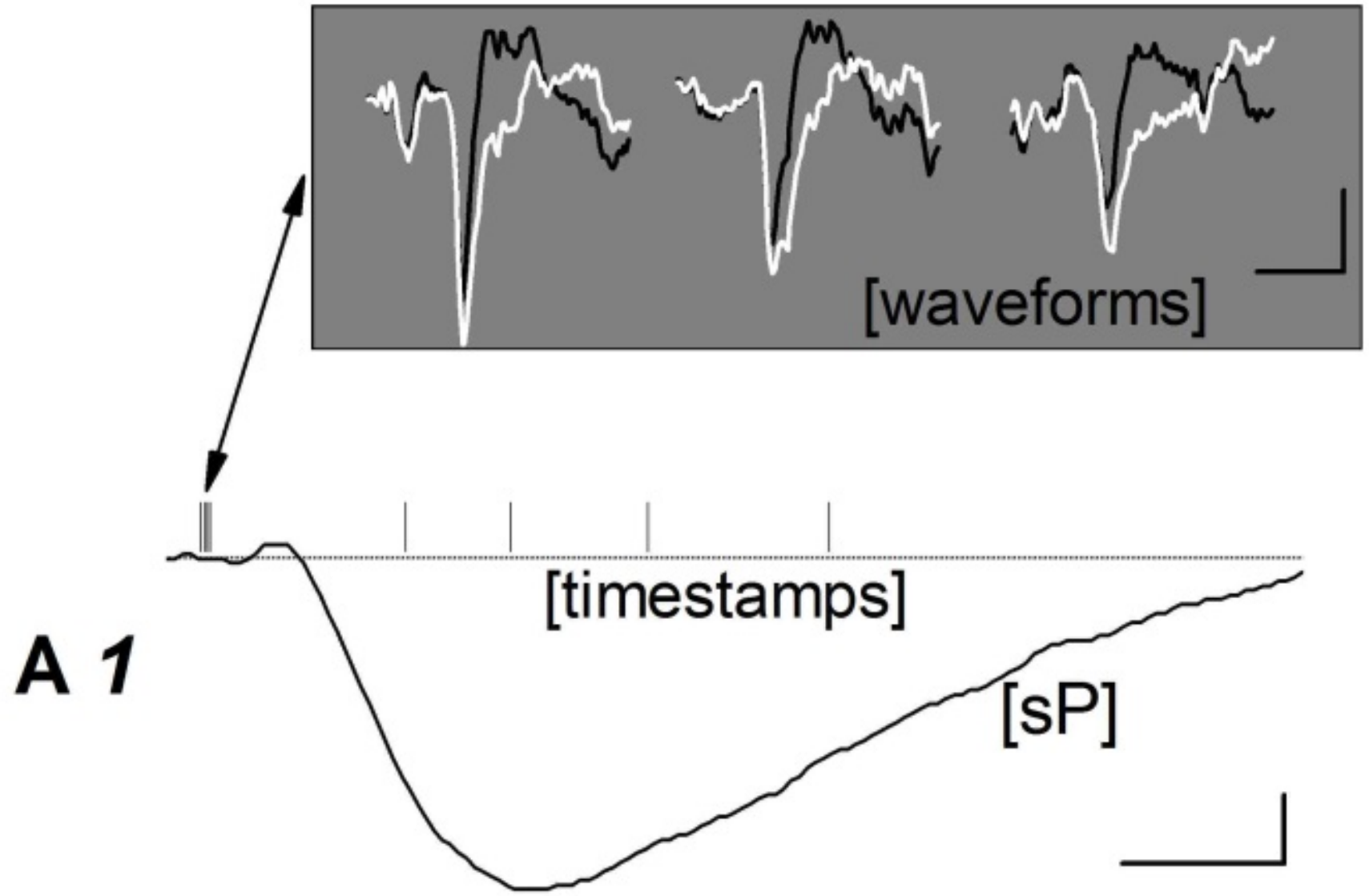
[waveforms]
[timestamps]
[sP]
A 1

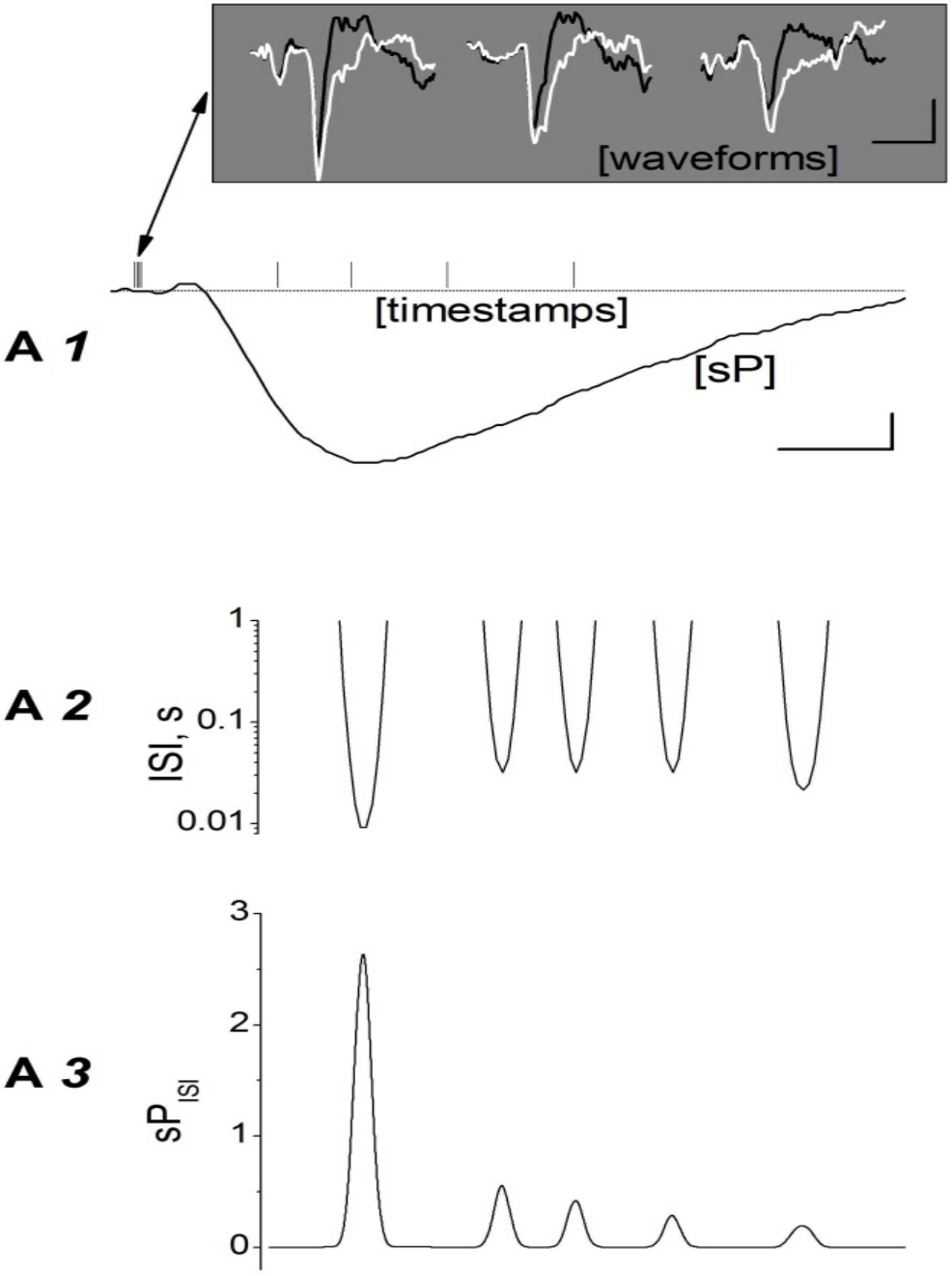

sP signals are strongly dependent on interspike intervals (ISI)

$$sP_{ISI} = |sP/ISI|$$

Barium, blocking Kir currents, strongly affects spike rates and PSD but not spike waveforms

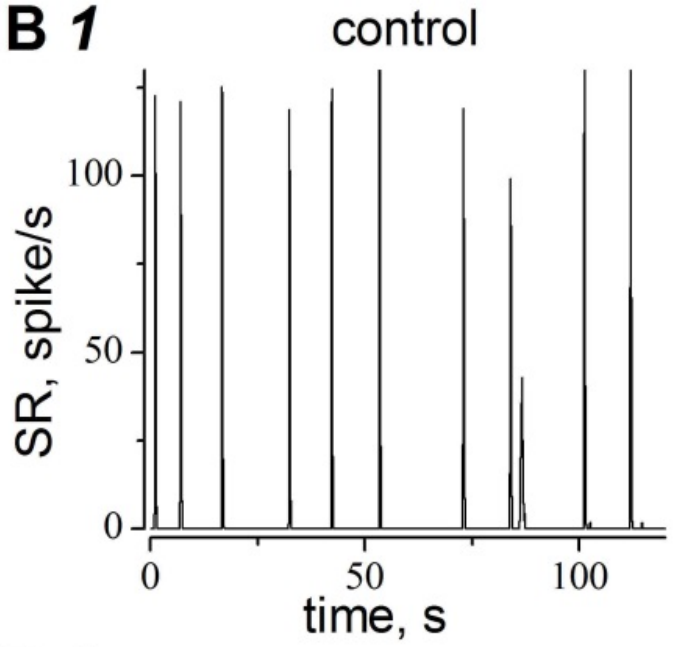

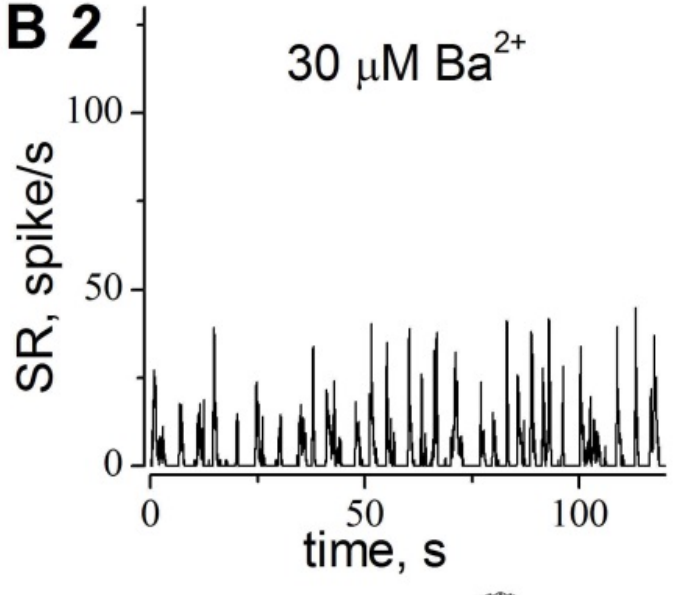

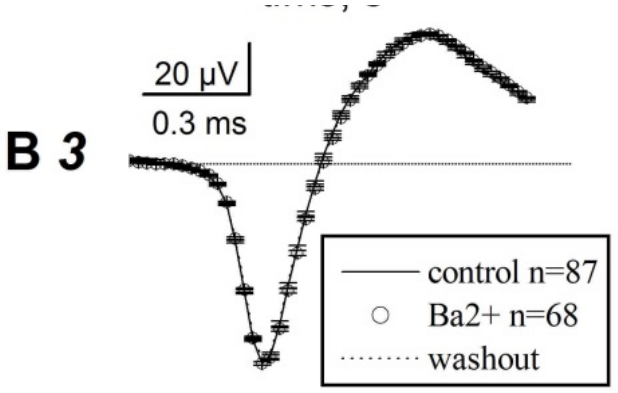

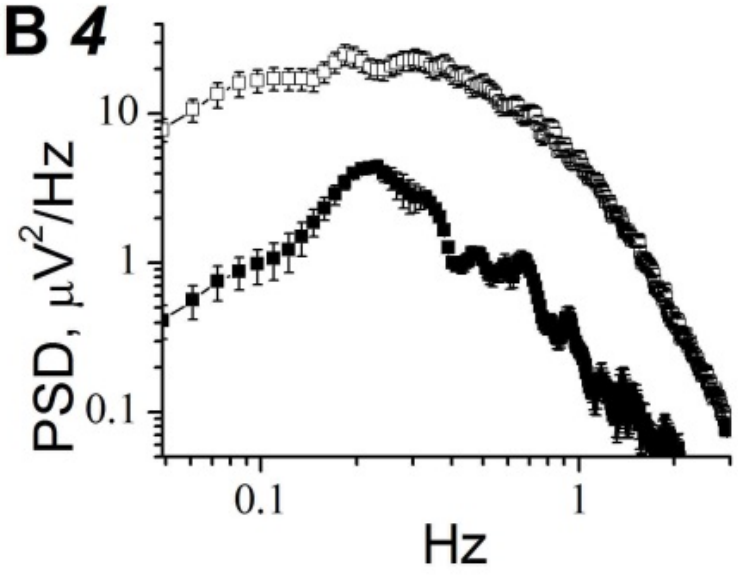

Days-in-vitro and network disinhibition affects sP waveforms and power spectra

Vertical bar 10 μV
Horizontal 0.5 s

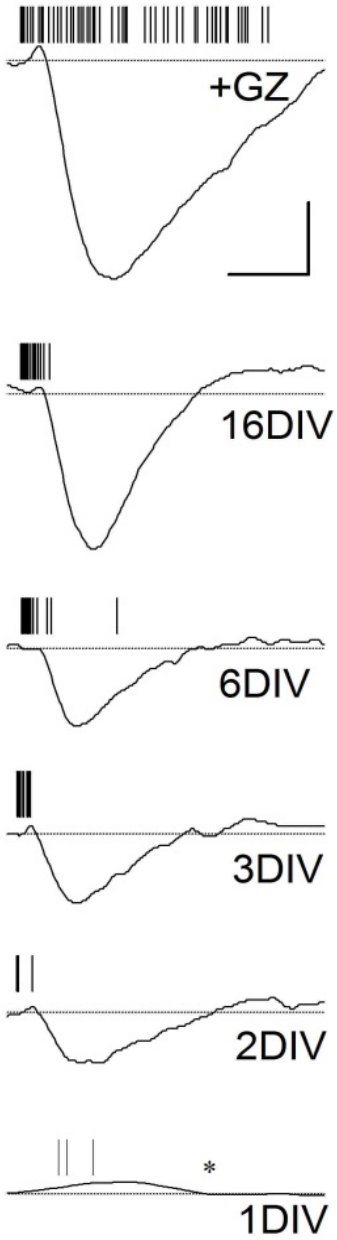

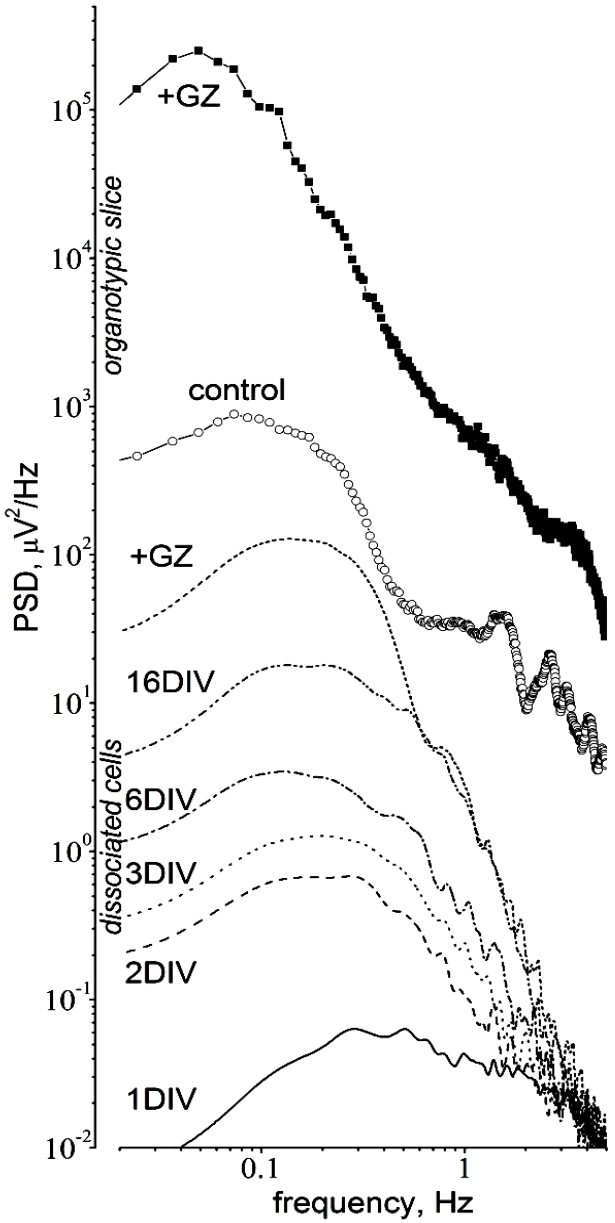

AraC blocking astrocyte's survival

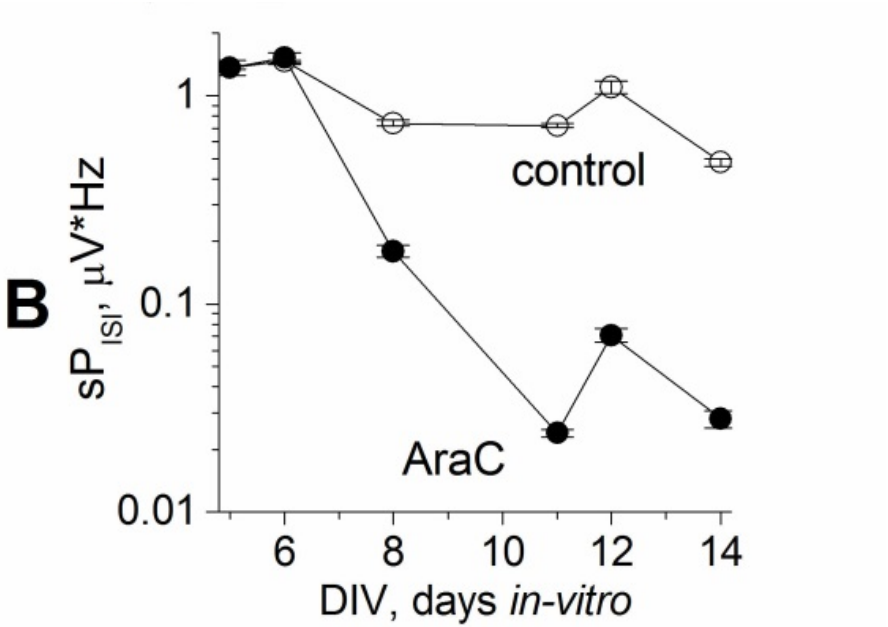

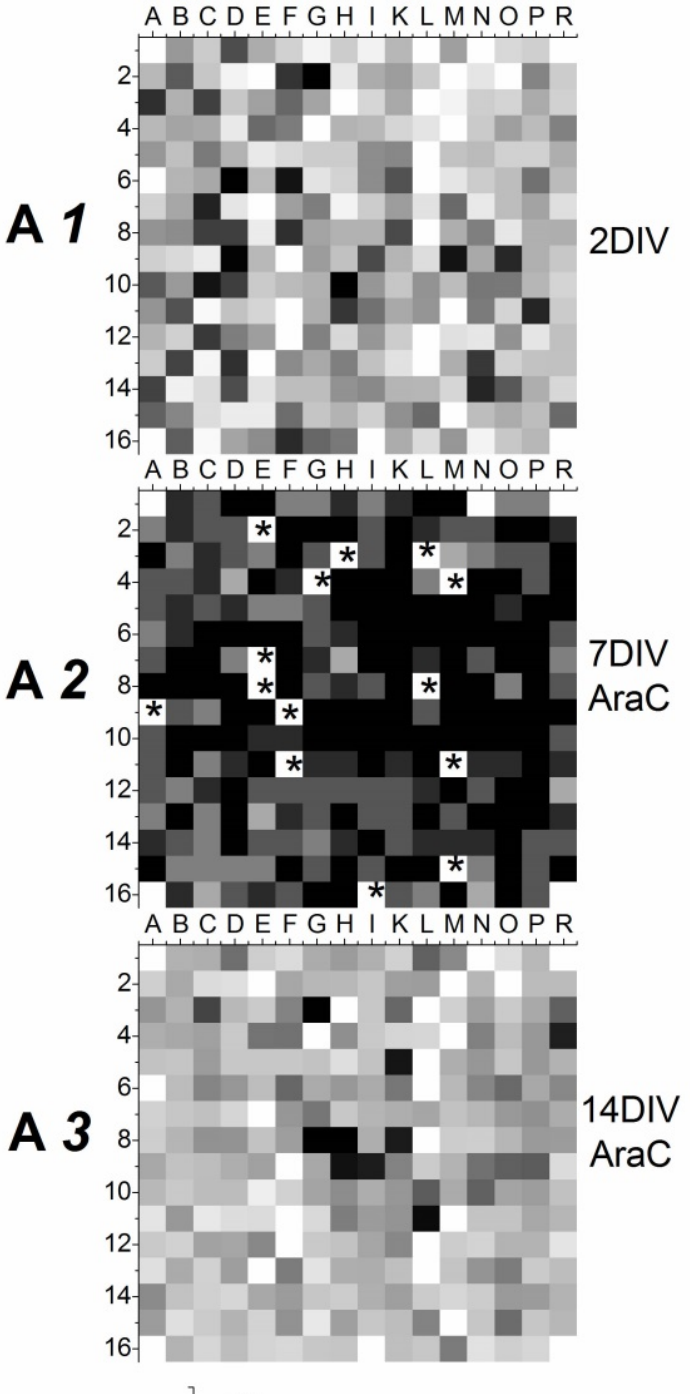

Same mea264
AraC from 7DIV
3.2x3.2 mm
grayscale
black **sP** = high
white = zero

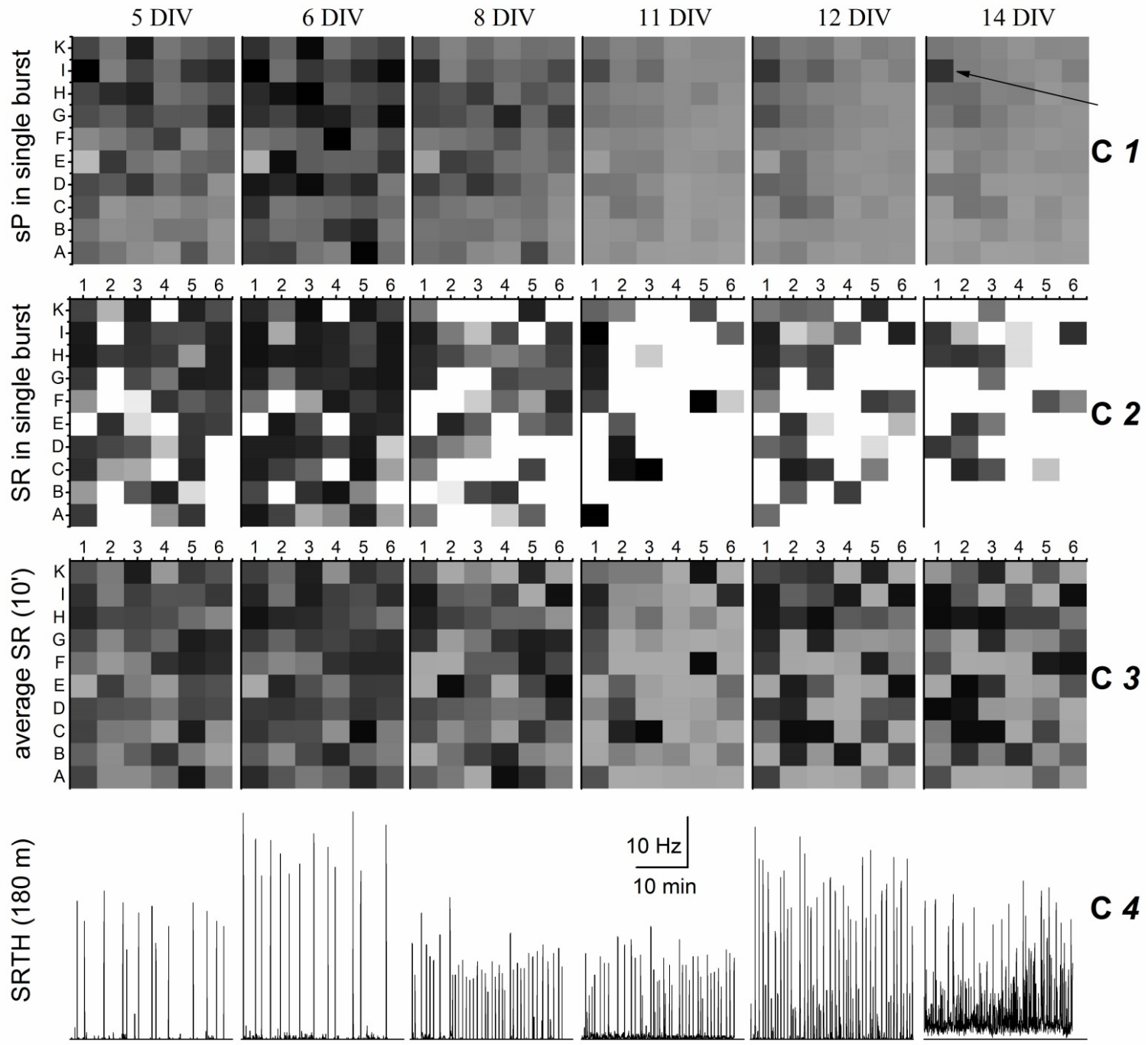

Same mea64
AraC from 6DIV
3x5 mm
grayscale
black **sP** = high
white = zero

mea64
spikes

Spikes (vertical bars) superimposed on outward- and inward-going **sPs**, same dish

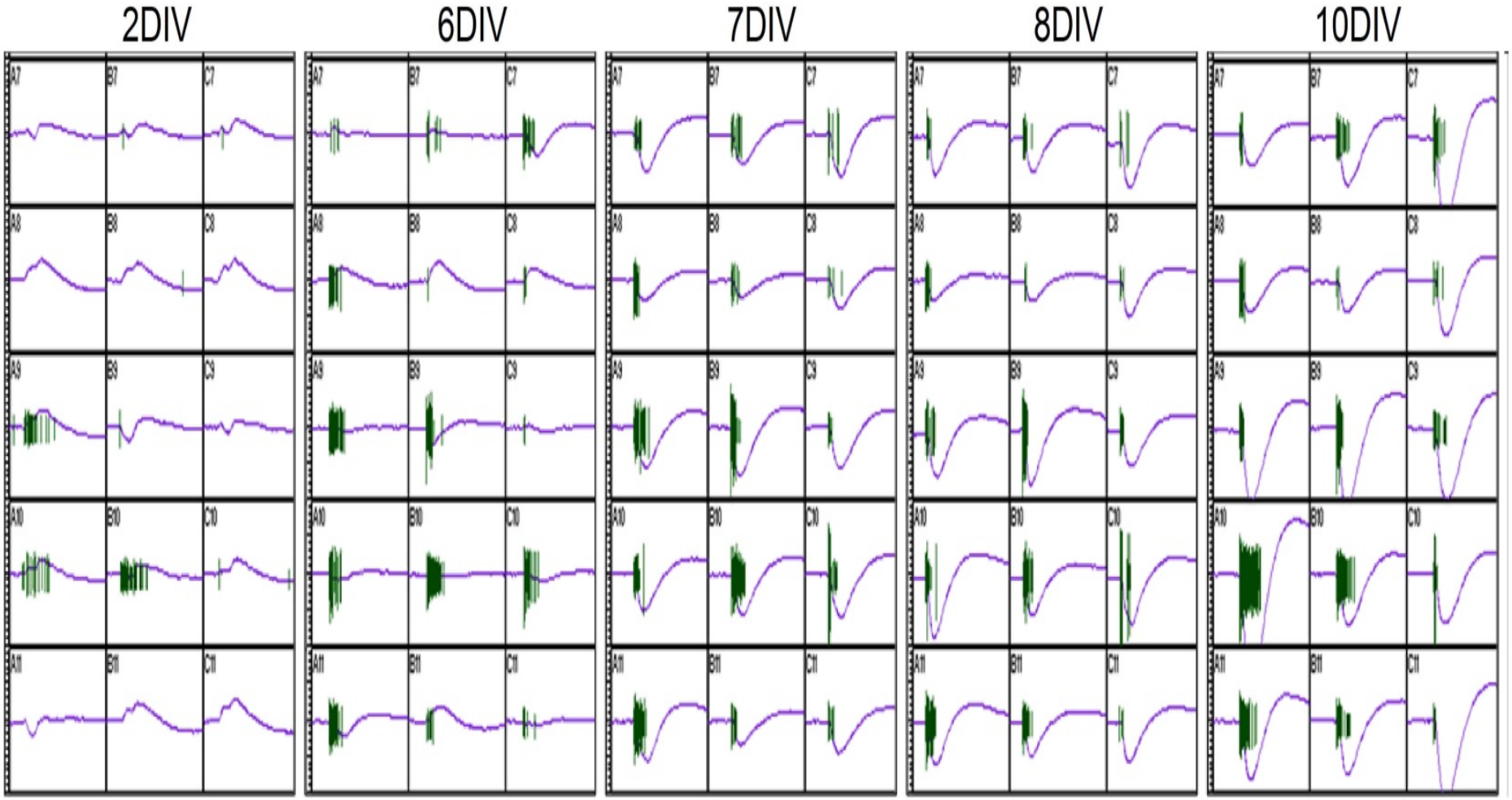

adjacent inward and outward sPs in electrodes with or without spikes

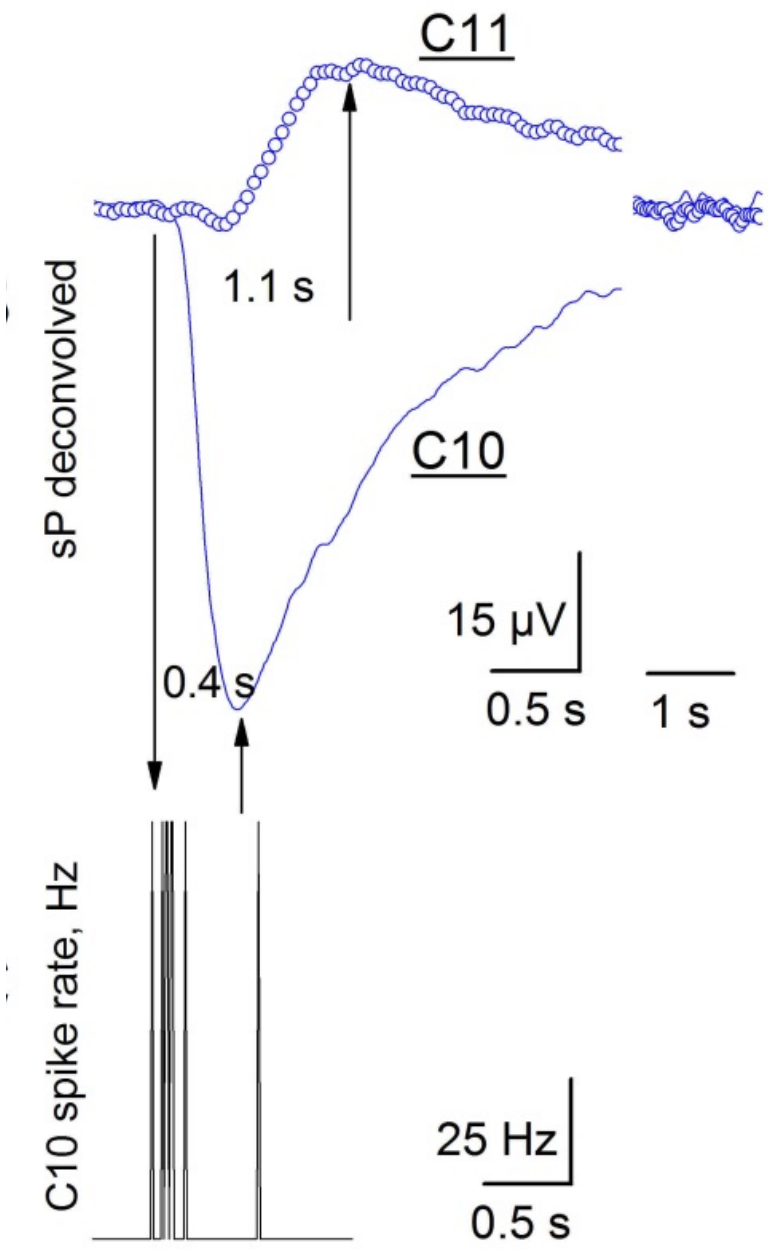

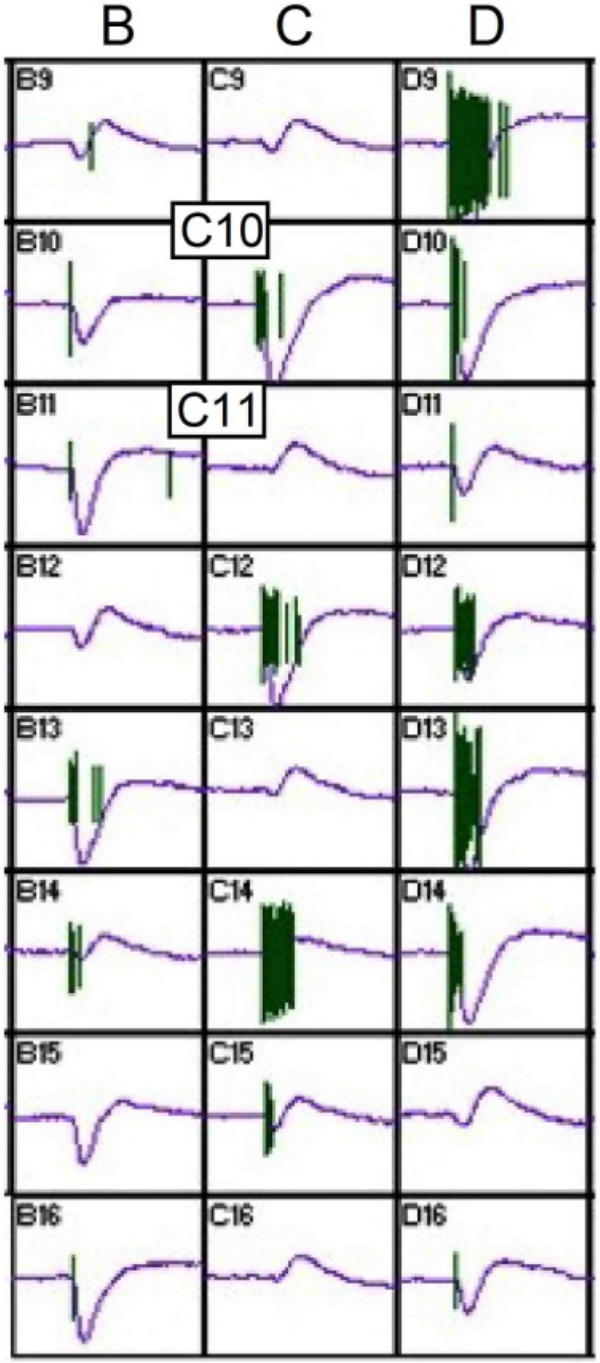

mea256 canale **LFP** spikes

demonstration of spatial K^+ buffering, organotypic cultured slice

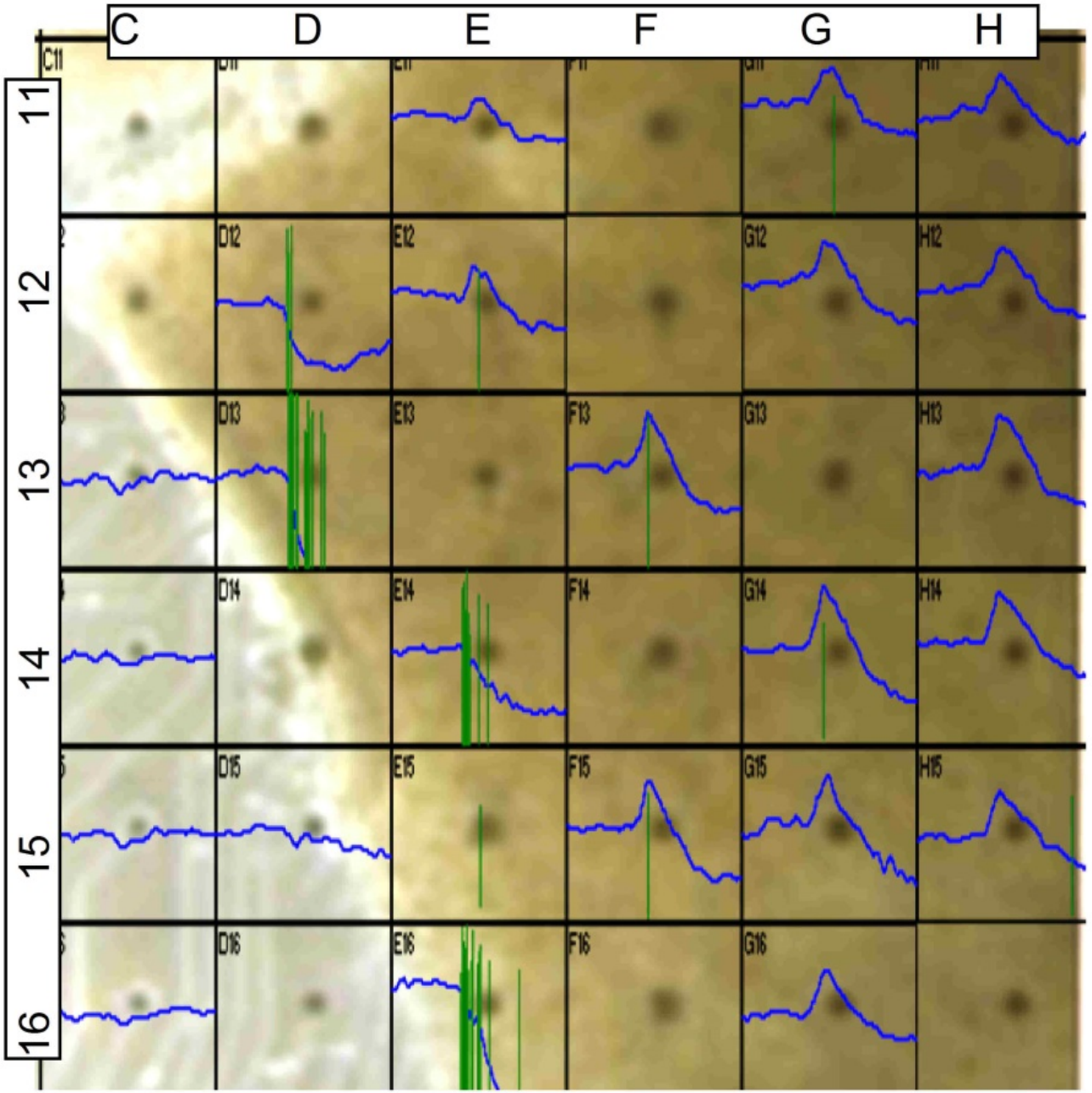

mea256
sP+spikes
1 burst

15-electrodes activity at 2DIV, 256mea

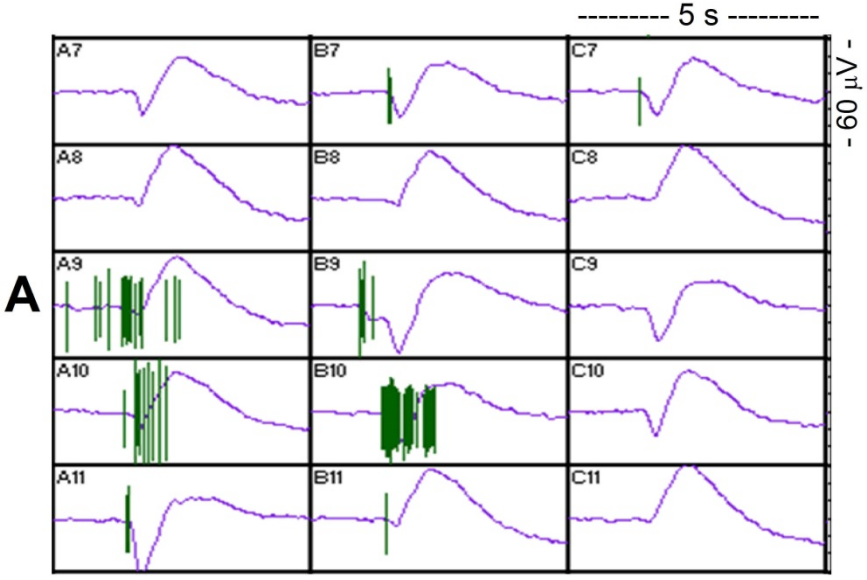

electrode B9, 2 types of spikes

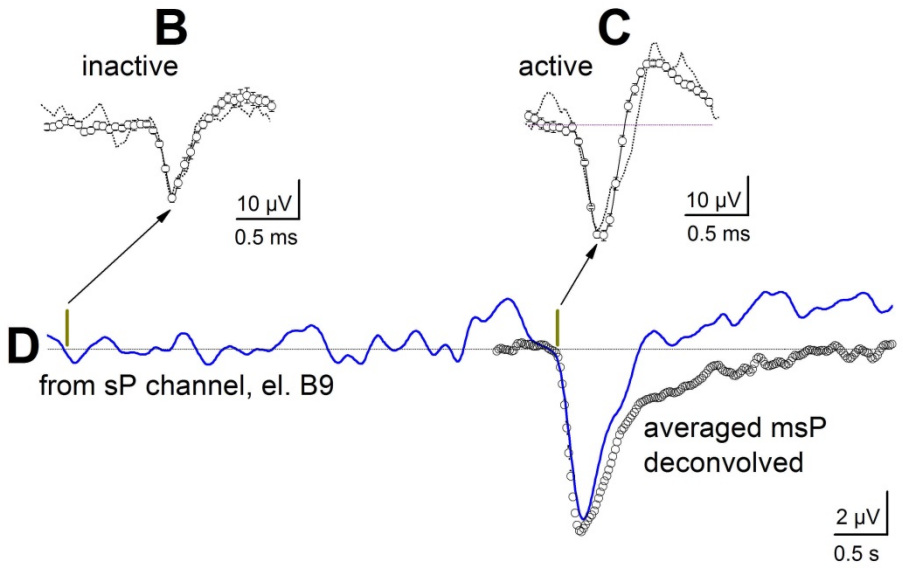

miniuture sP (msP)

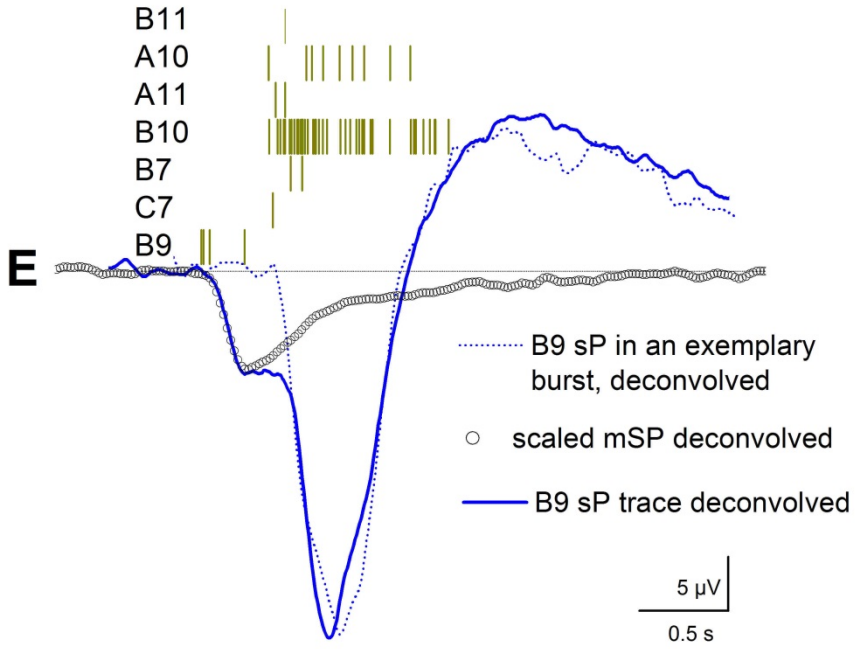

burst-induced sP effect
and
miniature sP effect

1956 Frankenhaeuser & Hodgkin, **predicted [K+]o change** and superimposed sP

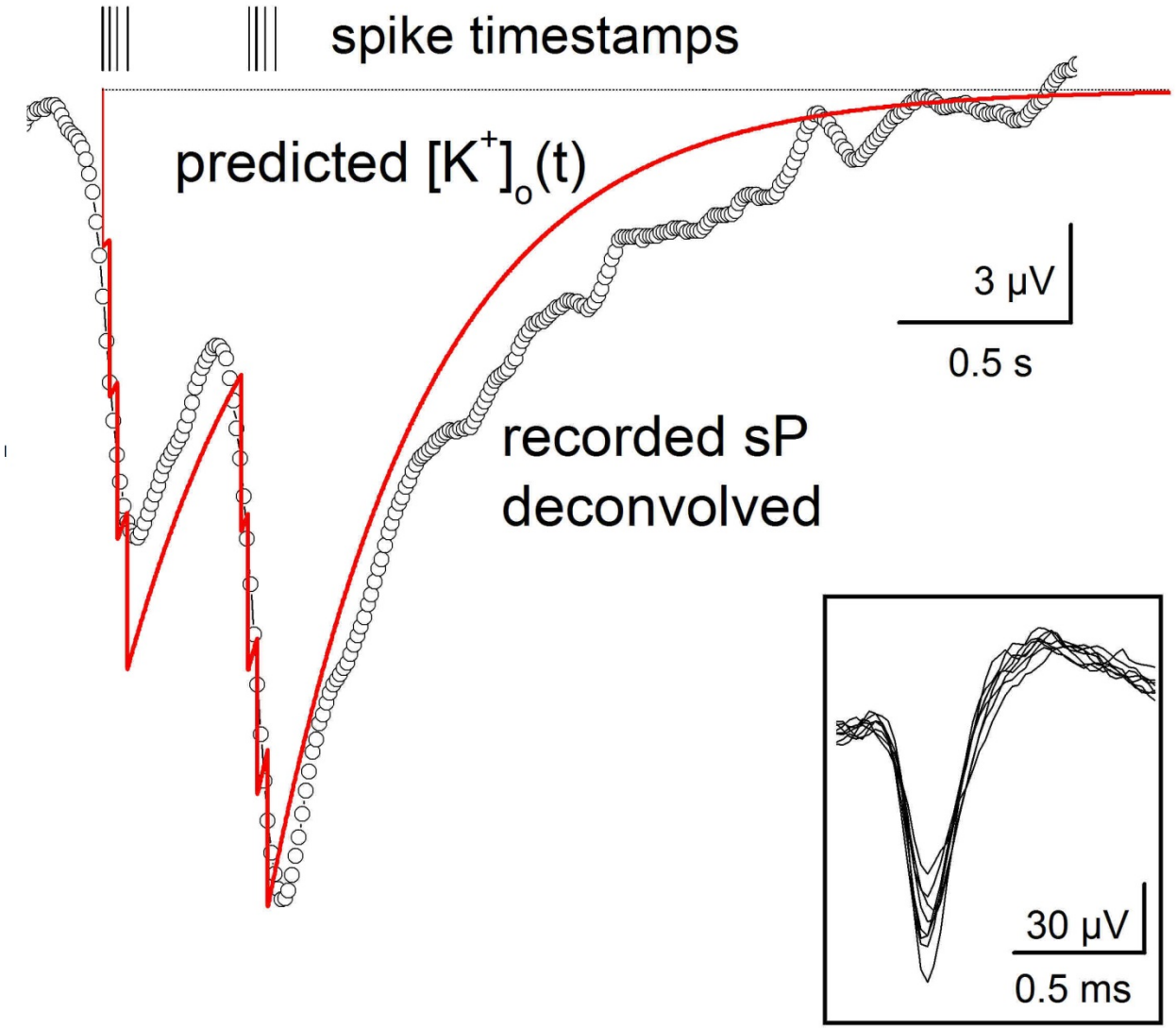

mea64
canale **sP**

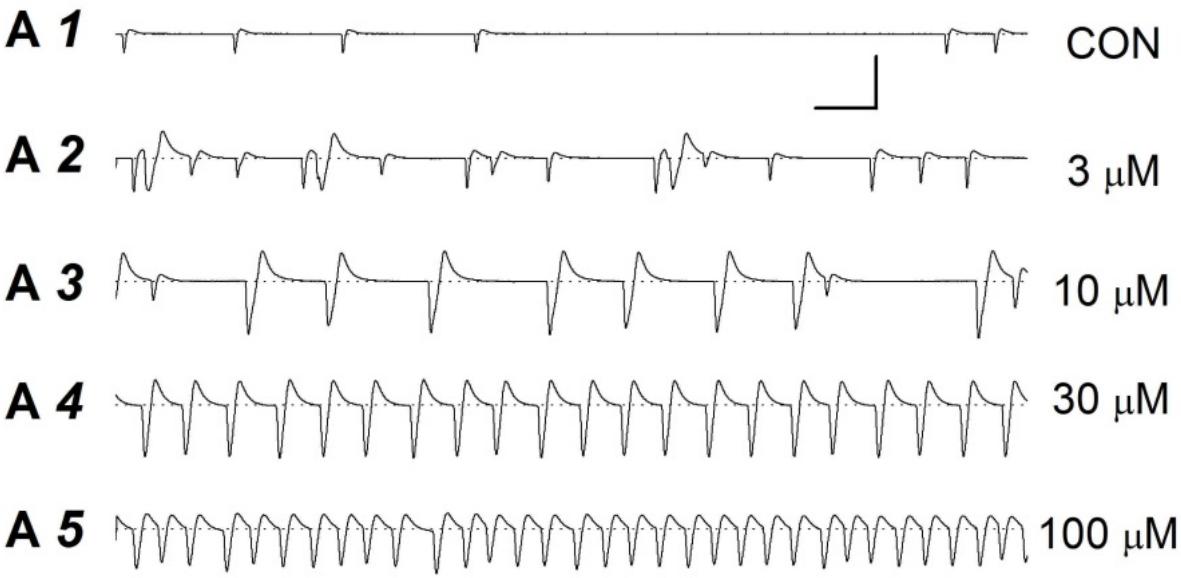

mea64
canale **sP**
63 bursts

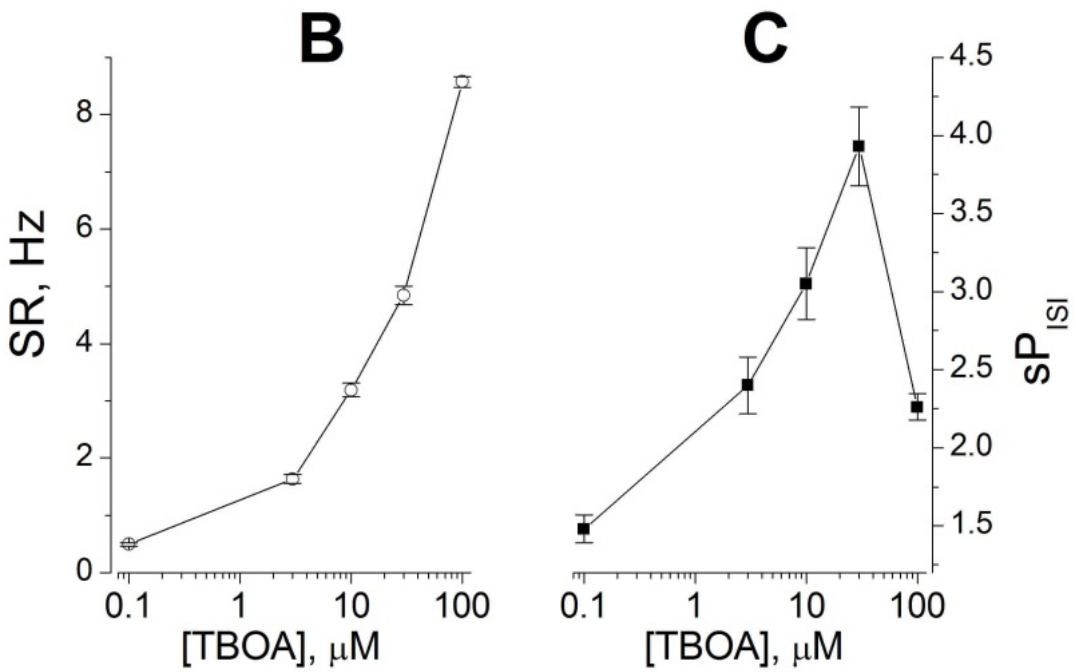

effects of increasing concentrations of TBOA, a drug blocking GluT
i.e. see:

Bergles DE, Jahr CE. Synaptic activation of glutamate transporters in hippocampal astrocytes. *Neuron* 19: 1297–1308, 1997.

Diamond JS, Jahr CE. Transporters buffer synaptically released glutamate on a submillisecond time scale. *J Neurosci* 17: 4672–4687, 1997.

Effects of TBOA and gabazin pharmacology on neuronal excitability and burst duration

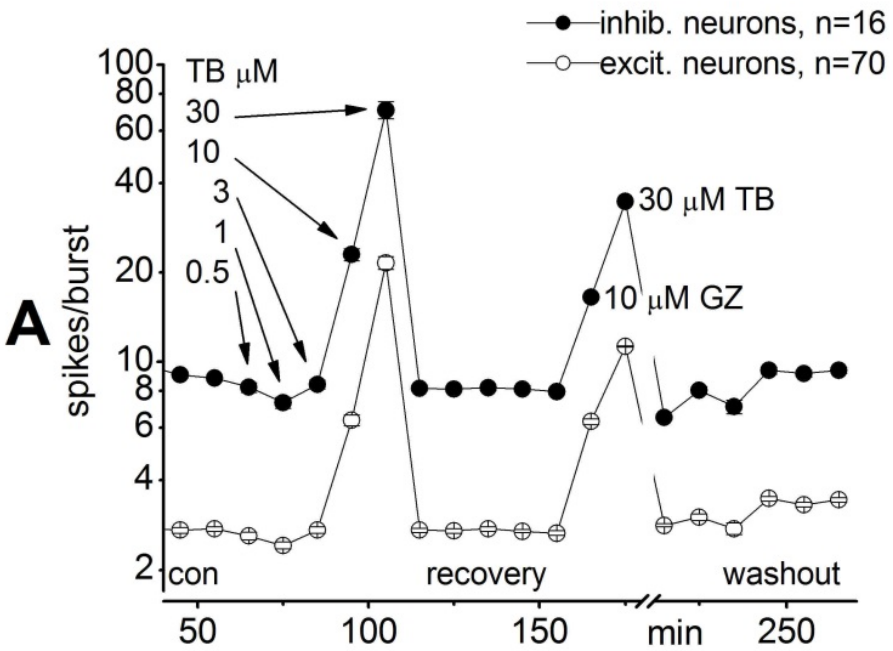

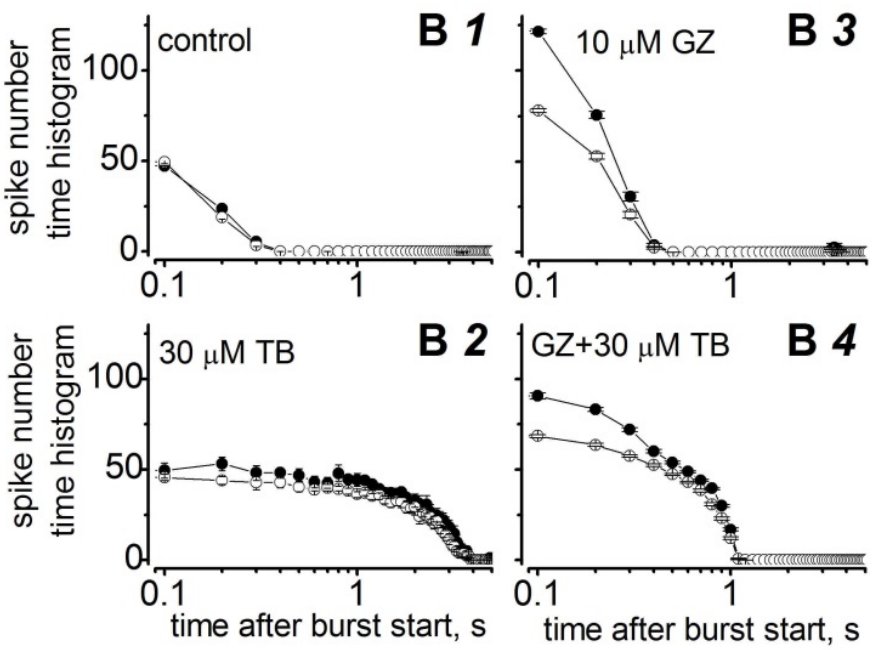

mea64
canale **LFP**
63 bursts

Effects of TBOA and gabazine pharmacology on waveform of **sP** and firing (same electrode)

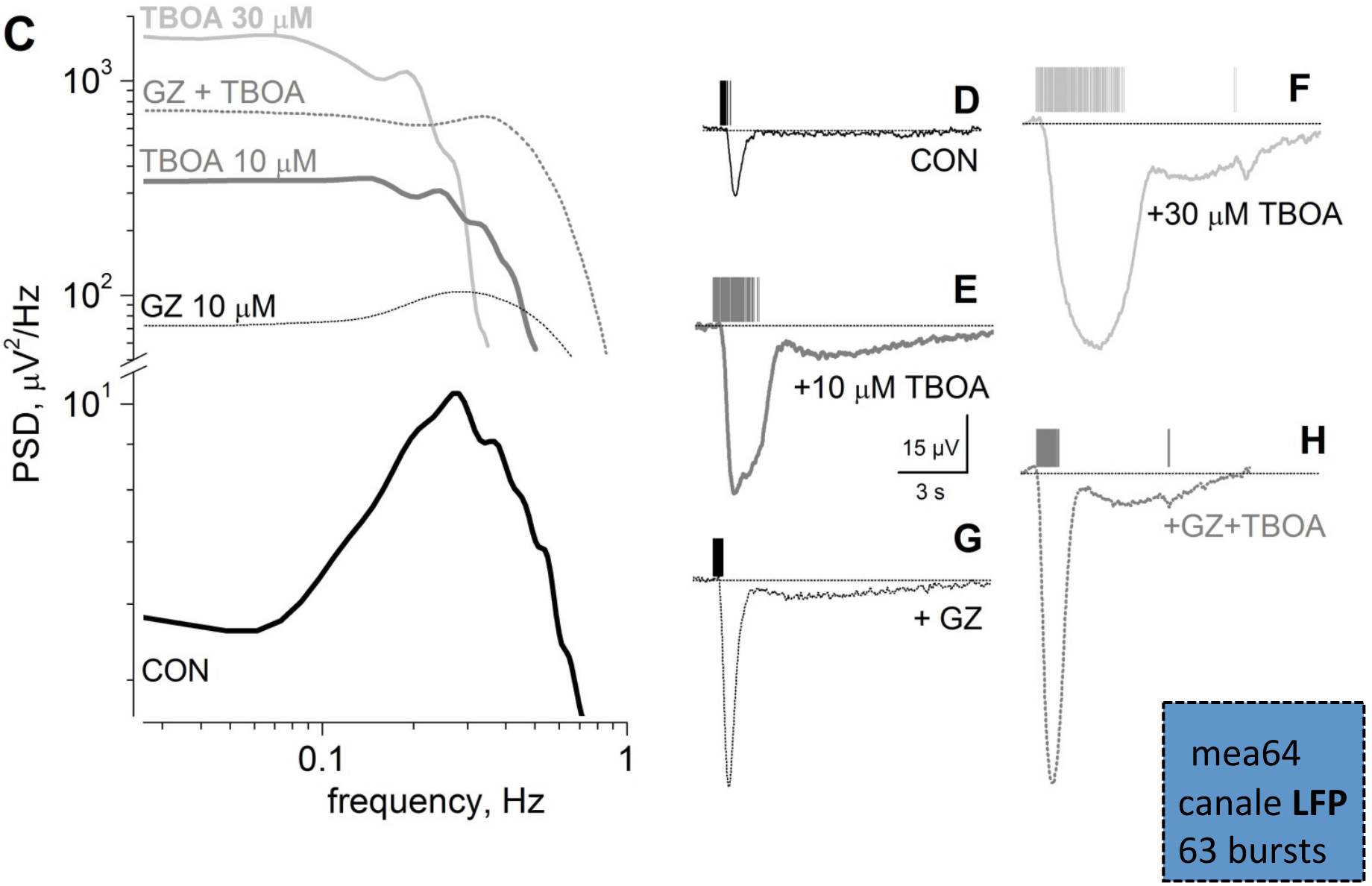

mea64
canale **LFP**
63 bursts

recordings of GluT currents from dissociated neurons during reverberating activity

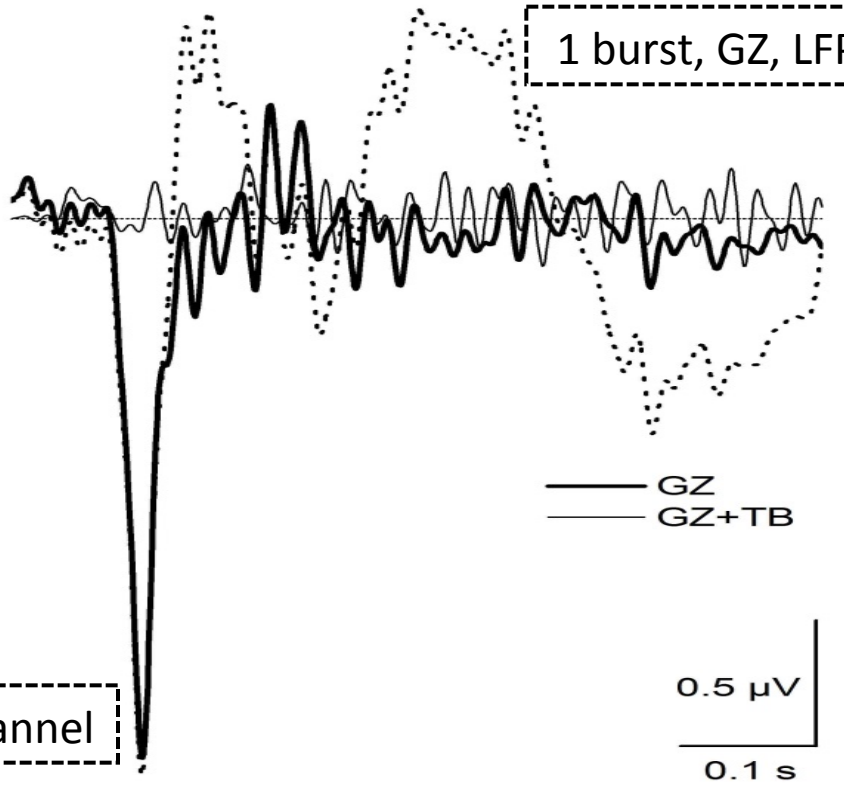

63 bursts LFP channel

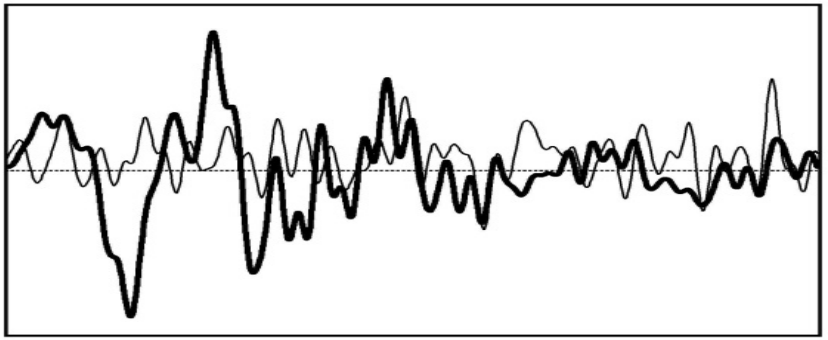

1 bursts, GZ, LFP channel

mea64
canale **LFP**

5 elettrodi adiacenti da mea256 spikes e canale **sP**

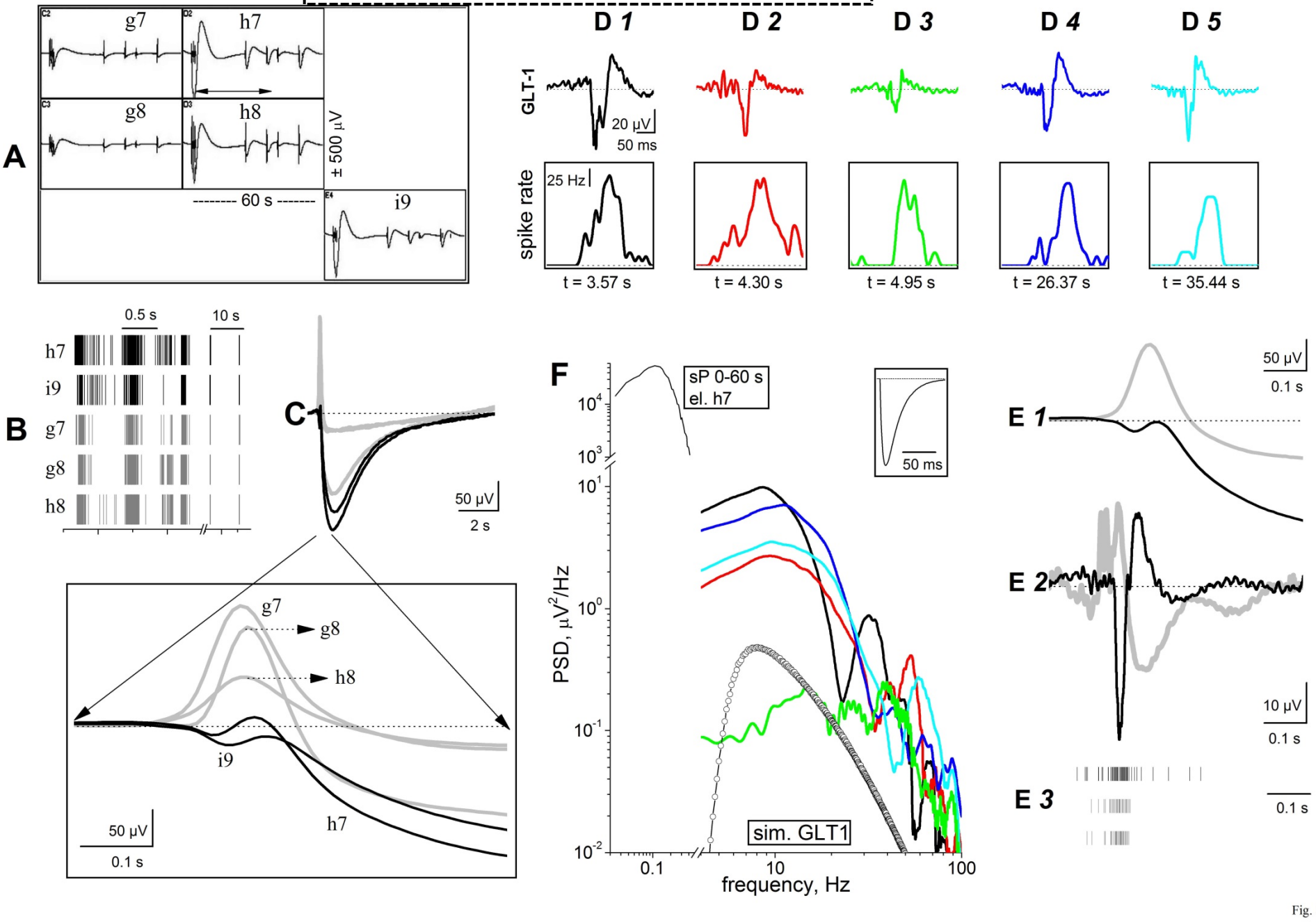

Fig. 8

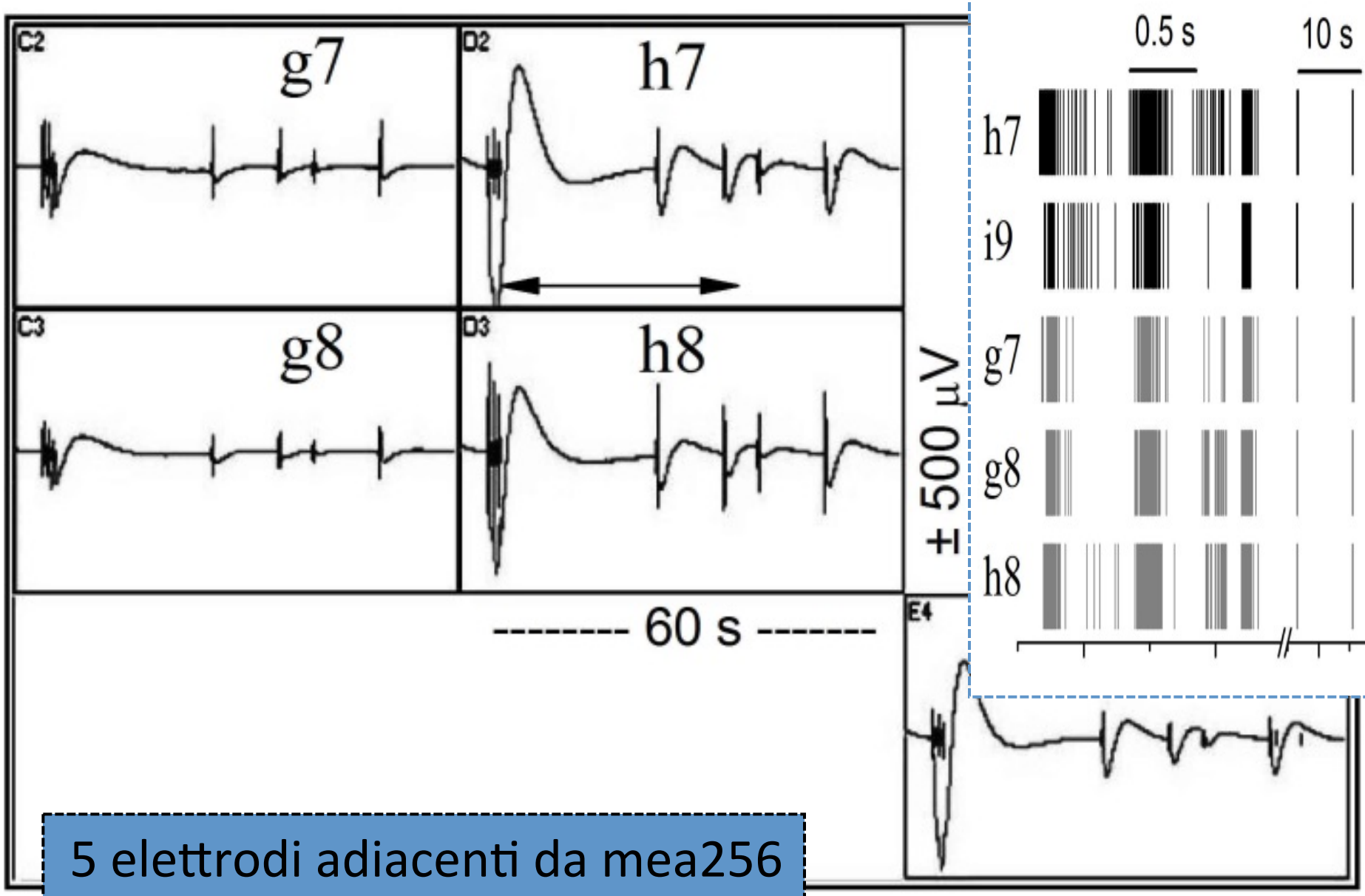

5 elettrodi adiacenti da mea256 spikes e canale **sP**

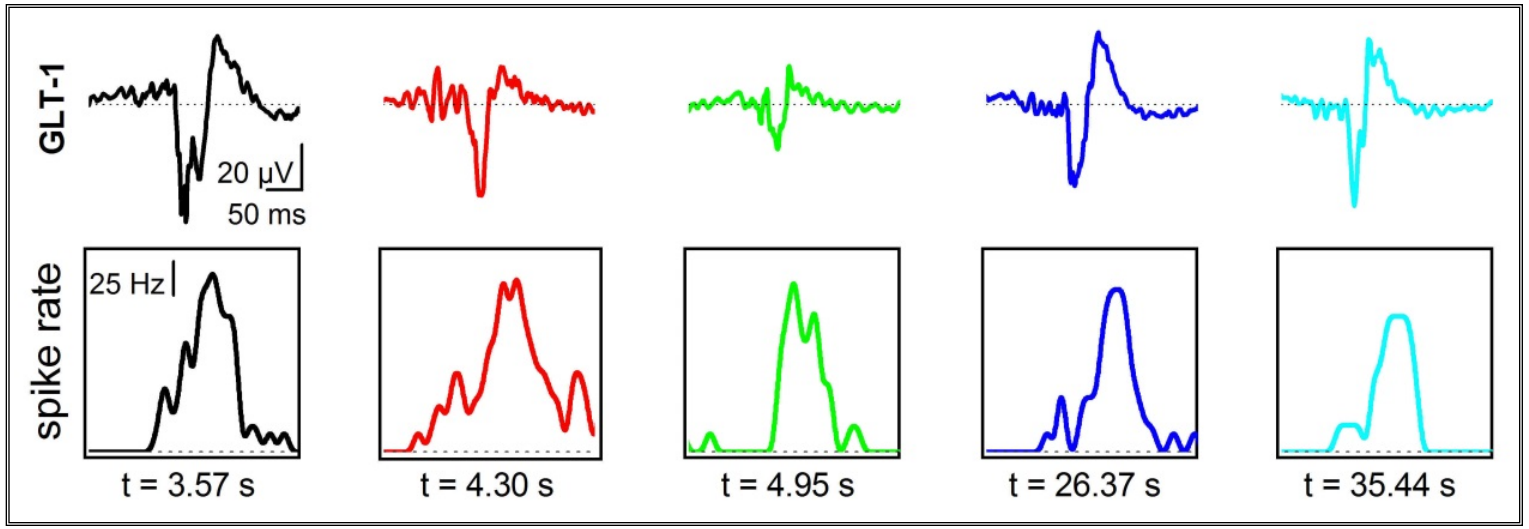

data from electrode h7 LFP channel

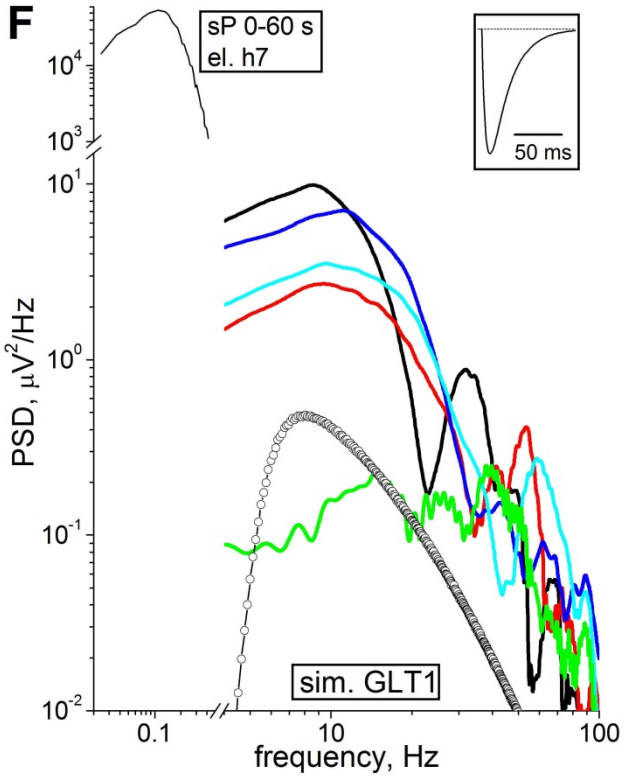

note that **sP** data from electrode h7 are 3 orders of magnitude higher

PSD data from electrode h7 LFP channel, same colors

mea256 canale **LFP** 5 bursts

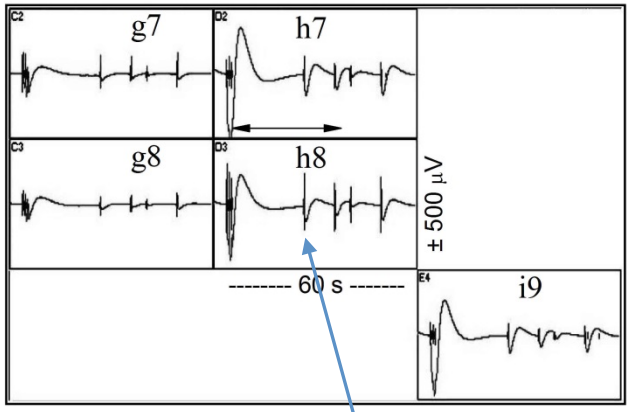

astrocytes far from g7, g8, h8
astrocyte near h7, i9

gray : mean of (g7+g8+h8)
black: mean of (h7+i9)

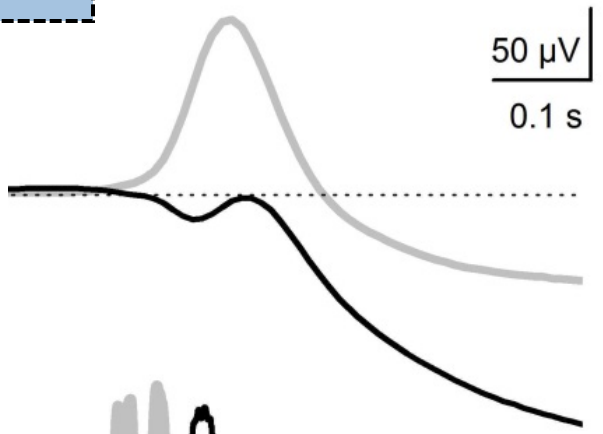

sP

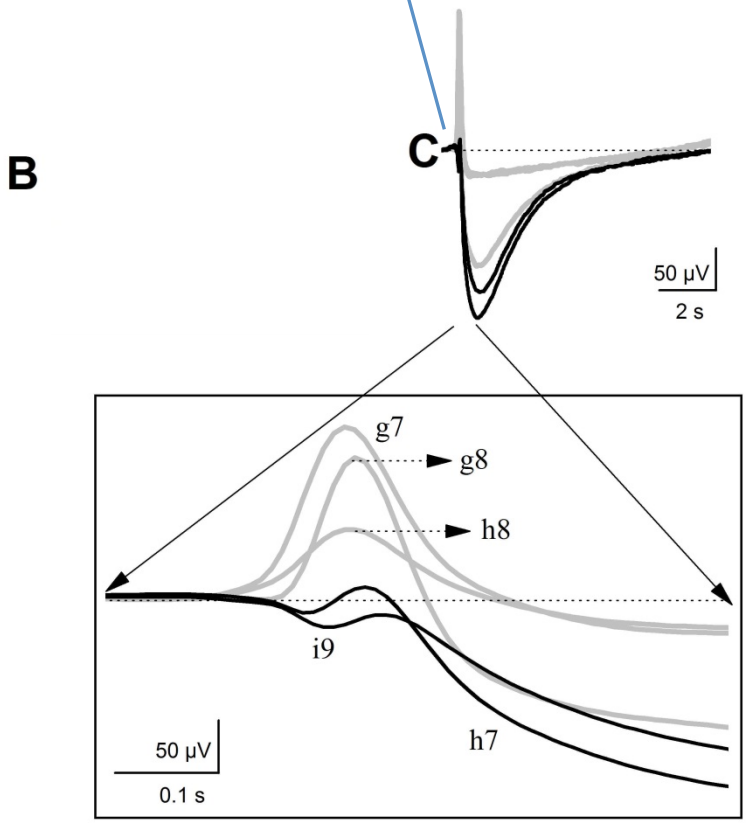

LFP

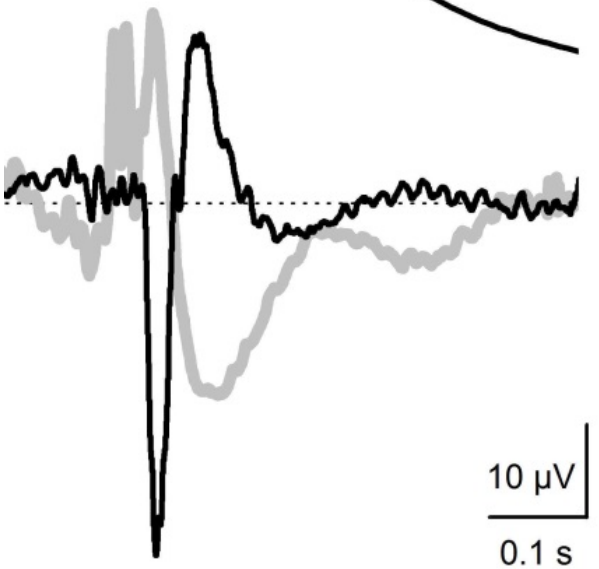

h7
g7
g8